



UNIVERSITY OF NEVADA - RENO - NEVADA - 89557

Mackay School of Mines
Seismological Laboratory

ANNUAL
TECHNICAL REPORT NO. 1

Telephone (702) 784-4975

03 December 1979

ARPA Order No.	3291
Program Code	7F10
Name of Contractor	University of Nevada, Reno
Effective Date of Contract	01 Oct 1978
Contract Expiration Date	30 Sep 1979
Amount of Contract Dollars	\$39,226
Contract Number	F49620-77-C-0070
Principal Investigator	William A. Peppin, 702-784-4975
Program Manager	William A. Peppin
Short Title of Work	Close-in and Regional Source Studies for Seismic Discrimination

Sponsored by

Advanced Research Projects Agency (DOD)

ARPA Order No. 3291

Monitored by AFOSR under Contract # F49620-77-C-0070

APPROVED FOR RELEASE;
DISTRIBUTION IS UNLIMITED (A)

DTIC
ELECTE
S JAN 24 1985 D
D

85 01 15 049

AD-A150 033

DTIC FILE COPY

TABLE OF CONTENTS

	Page
TECHNICAL REPORT SUMMARY	1
1. COPE FOR SOURCE INVERSION	2
2. DEVELOPMENT ON THE SEISMOLOGICAL LABORATORY COMPUTER SYSTEM	4
3. SEISMIC DISCRIMINATION AT NEAR-REGIONAL DISTANCES	5
3.1 PN versus Rayleigh Discrimination at Jamestown	5
3.2 P versus S Discriminant at Jamestown	8
3.3 Seismic Discrimination at Jamestown: Summary	11
4. SEISMIC DISCRIMINATION AT REGIONAL DISTANCES USING PN	13
5. ANALYSIS OF CLOSE-IN ACCELEROMETER RECORDS OF MEGATON EXPLOSIONS	16
5.1 Source in a Layer	17
5.2 Source Below a Single Layer	18
5.3 Helmberger-Hadley Model	19
5.4 Extended Helmberger-Hadley Model	19
6. PN DISCRIMINATION IN A SHIELDLIKE ENVIRONMENT	21
7. PERIPHERAL STUDIES OF INTEREST TO THIS CONTRACT	22
7.1 Digital Data Acquisition and Spectral Corner Frequencies	22
7.2 Analysis of Explosion Surface Waves for Phase Velocity	24
REFERENCES CITED	25

Accession For	
NTIS GRA&I	<input checked="" type="checkbox"/>
DTIC TAB	<input type="checkbox"/>
Unannounced	<input type="checkbox"/>
Justification	
By	
Distribution/	
Availability Codes	
Dist	Avail and/or Special
A/1	



**BEST
AVAILABLE COPY**

TECHNICAL REPORT SUMMARY

This contract has as its primary objectives the investigation of close-in and near-regional (i.e., 0 to 600 km) seismic data for the purpose of implementing and understanding seismic discriminants, by which we mean any methods based on the analysis of seismic waves which permit unambiguous identification of seismic explosions as either underground explosions or earthquakes. Efforts during this contract period have emphasized the development and testing of a new and rather sophisticated inversion method for seismic sources, the seismic moment tensor method, whose use was first attempted by Stump and Johnson (1977) at these distance ranges. Material presented includes the following. In Section 1 we present comments about the development of a major new computer program specifically built to produce the more realistic Green's functions needed for moment tensor analysis. Section 2 is a discussion of developments accomplished on the Seismological Laboratory computer system in support of this contract. In Section 3 is presented a discussion of two near-regional discriminants based on new wideband data: the PN-Rayleigh discriminant of McEvilly and Peppin (1972), and an S to P ratio method that has been investigated under different names by several authors. In Section 4 is described an attempt to effect seismic discrimination through use only of the PN phase using the wideband three-component data of the Lawrence Livermore Laboratory. In Section 5 Green's functions for moment tensor analysis of the close-in JORUM and HANDLEY accelerometer data are discussed. This work extends the previous work of the author and a number of others on this important data set. In Section 6 we discuss efforts directed at testing the PN discriminant described in Section 4 over a "shieldlike" structure based on large underground explosions in Missouri. In Section 7 we discuss some work that is peripheral, but related to this contract involving the study of the

earthquake source mechanism, including the recent series of earthquakes along the eastern Sierra front and Rayleigh wave dispersion on the test site.

1. CODE FOR SOURCE INVERSION

Midway through this fiscal year I made operational a code to compute ground displacement from general seismic sources. This code, named MEXEC, is a full generalization of the earlier one used for the computation of ground motion from explosion sources. The output is directly compatible with Brian Stump's moment tensor inversion code (Stump and Johnson, 1977; Stump, 1979). The general philosophy of this approach to seismic sources is distinct from the more commonly-applied ones. Usually the assumption is made that the source is either a pure explosion or a pure earthquake with fault planes having some orientation; then some method such as generalized ray theory is used to propagate energy from this source to the receiver (see the treatment by Johnson and McEvelly, 1973 for example). In moment tensor analysis, we make no such assumption. Rather, appealing to the theory of Burridge and Knopoff (1964), we assume the source to be representable by a system of buried body forces. These body forces are expanded about a convenient point in a series known as the moment tensor representation (Stump and Johnson, 1977). Then, observed seismograms are fitted by such a linear combination of these force moments that the residual of predicted from observed seismograms is minimized in a least-squares sense. This procedure effects an inversion for the components of the "seismic moment tensor", which for small sources can be taken as particular linear combinations of the derivatives of the Green's function for the problem. What is significant about this procedure is that no a priori assumption about the source is made with regard to its identity as an explosion or earthquake: that information emerges from the

inversion together with error estimates as to how precisely the moment components are known. In other words: inversion is done and we can say that a certain percent of the source (with some uncertainty) is an explosion, some other certain percent is contained in, e.g., a dip-slip earthquake, and so forth. This is a statement of the central problem of seismic discrimination, and so is the natural method to use. To date, no work on seismic discrimination has been done at the close-in and near-regional distance ranges using the moment tensor method. The MEXEC code and a host of data collected by this author have been brought together in an effort to test thoroughly the efficiency of the method and, it is hoped, gain some new insight into the nature of the seismic source.

In the course of writing the MEXEC code, I have redesigned the parts where the source terms are entered in such a way that computation of all of the higher-order moment source types is trivial. Although only those of first order are computed in the present version of the code, it is a matter of changing a few lines of FORTRAN in a single subroutine to treat any of these components. A considerable time during this contract period was also spent in documenting the code and some of the more sophisticated numerical difficulties that have come up. As a result of this effort, I believe that the code is finally working correctly. Some quite critical tests have been made although I cannot yet certify the correctness of the code. A central problem in bringing up this code was a collection of quite difficult numerical problems that had to be overcome. The Cagniard-deHoop method permits an elegant and simple way to write down the solutions to difficult problems in wave propagation; however, transforming this deceptively simple expressions into an operation computer code is altogether another matter (the solutions were developed in about 300 hours of work, but the program has consumed no less than 5,000 hours of development time).

I should emphasize why I endured such a long development effort when generalized-ray codes were available from groups at Caltech and elsewhere. The answer is twofold: first, I never found the documentation provided by the Caltech group sufficient to understand completely what was being done, so I would have had great difficulty understanding their codes; second, my code differs from the more usual ones involving generalized-ray analysis in that it is exact at all distance ranges, no approximation having been made anywhere in the analysis. This permits investigations of seismic records at very close distances to the source without the worry of having to know which terms in the asymptotic series to retain.

Cooperative studies are underway with Lawrence Livermore Laboratory, where I will again be a consultant for the time period of this contract. MEXEC has been placed on LTSS at Livermore, and on the Prime computer in the Geophysics division there. It has also been made operational at Kirtland Air Force Base for use by Brian Stump for projects involved in his responsibilities and for moment tensor analysis. In Sections 4 and 5 are presented examples of output from the MEXEC code.

2. DEVELOPMENTS ON THE SEISMOLOGICAL LABORATORY COMPUTER SYSTEM

During this contract period a considerable body of FORTRAN software was created for digital signal processing on the Seismological Laboratory PDP 11/34 computer. This software was developed in the course of the completion of three Master's degrees by grad students, and for the processing of the data from the digital event recorders developed with support from AFOSR. Under Keith Priestley's contract with AFOSR, codes were developed for determining the structure of

the Basin and Range using surface-wave analysis, gravity, and seismic refraction profiles. In support of this contract, I have developed the software for processing records obtained from the Berkeley tape system (see Section 4). The system has been upgraded by acquisition of a maintenance contract from Digital Equipment, by implementation of the new release of RSX11-M, purchase of a fast compiler FORTRAN IV PLUS, and a remote hardcopy device for the Tektronix graphics terminal. The computer has served all of our real-time and other processing needs very well, and we anticipate no significant need of additional hardware and software support for the objectives of this contract. During the contract period our computer systems analyst position changed hands from Ron Sheen to Dennis Ghiglieri, who has proven an able replacement. The staff uses the computer almost daily, a clear testimonial to the simplicity and usefulness of the machine.

3. SEISMIC DISCRIMINATION AT NEAR-REGIONAL DISTANCES

3.1. PN versus Rayleigh Discrimination at Jamestown

McEvilly and Peppin (1972) and Peppin and Mc Evilly (1973) found a successful seismic discriminant between underground nuclear explosions at Nevada Test Site (NTS) and earthquakes. Making use of the wideband systems at Berkeley, Mina, and Elko, Nevada, Kanab, Utah, and Landers, California (distance range 200 to 660 km from NTS), almost all events were successfully separated by a good margin, providing one of the few effective near-regional discriminants. The discriminant compared the maximum amplitude of the PN phase in a pass band 0.5

to 5 Hz with maximum filtered (0.02 to 0.01 Hz) Rayleigh wave motion. Surface waves were detectable for explosions down to a body-wave magnitude of about 3.6, and for earthquakes somewhat lower.

Now the discriminant was found to be effective at Berkeley and Mina, both northwest of the test site, but less effective in the azimuths towards Kanab and Landers (i.e., due east and due south from the test site). It is of interest to know if this discriminant works in general. Therefore, when the University of California at Berkeley commenced operation of a wideband system at Jamestown, also NW of the test site and in the Sierra foothills, an opportunity was provided to study the discriminant at yet another wideband station. By this time sufficient data has been recorded on the Jamestown system to test the PN-Rayleigh discriminant rather thoroughly. It is noteworthy that the Jamestown station simulated an SRO site, because the data, although recorded analog, are kept for a variety of gains and bandwidths. Thus, data is available for earthquakes anywhere in the western United States in the magnitude ranges from about 3 to 6.5. The pass bands used for the analysis described here were the highgain shortperiod (0.2 to 1.0 ^H Hz, "SPZ"), wideband velocity (0.025 to 10 Hz, 0.5 volts/micron/sec, "BBV"), and wideband displacement taken at two gain levels (0.025 to 10 Hz, 0.5 or 0.0025 volts/micron, "DHG" or "DLG" for high and low gains, respectively). Whole-record data for explosions in the local magnitude range 3.0 to 6.5 is available for the continuously-recorded data set running from 1975 to the present time.

From Jun 1975 to Feb 1979 $\frac{M}{J}$ events were selected for analysis. As in the previous studies, the primary difficulty is in finding suitably-recorded earthquakes on the test site. There was none at all on the test site except hole

collapses. Consequently, following the method of McEvilly and Peppin (1972), a search was made for events at around 400 km from Jamestown. Earthquakes found spanned a large range of azimuths from NW (near Shasta Dam, California) through northern and central Nevada, Death Valley, China Lake, and the San Fernando Valley (about 225 degree range of azimuths). Of the events selected 48 had PN and Rayleigh wave signals that could be studied (Table 1). The smallest magnitudes were slightly below ML 4.0 (which is not as low as deemed desirable for seismic verification purposes).

Figure 3.1 is a plot similar to those presented by McEvilly and Peppin (1972) and Peppin and McEvilly (1973). Numerals by each symbol are event numbers in Table 1. Surface-wave amplitudes were read on either the BBV, DHG, or DLG channels off visicorder playouts from analog tape after filtering (0.02 to .10 Hz, 48 db/octave rolloff). Presented for a Rayleigh wave measurement is the maximum peak-to-peak amplitude on the filtered trace of the DHG channel. For some cases (asterisks in Table 1) it was impossible to obtain a reading on the DHG channel. In that case the reading was obtained either from DLG through the static gain adjustment between them of 200, or through an empirical adjustment

$$\text{DHG} = \text{BBV}/(11.1 \pm 2.6)$$

obtained for the 22 events having a useable surface wave on both the DHG and BBV channels. Presented for the PN measurement is the maximum peak-to-peak amplitude determined on SPZ, filtered 0.5 to 3.0 Hz (24 db/octave rolloff). The larger events clipped on this trace, so an empirical adjustment was made from the BBV and DHG traces as

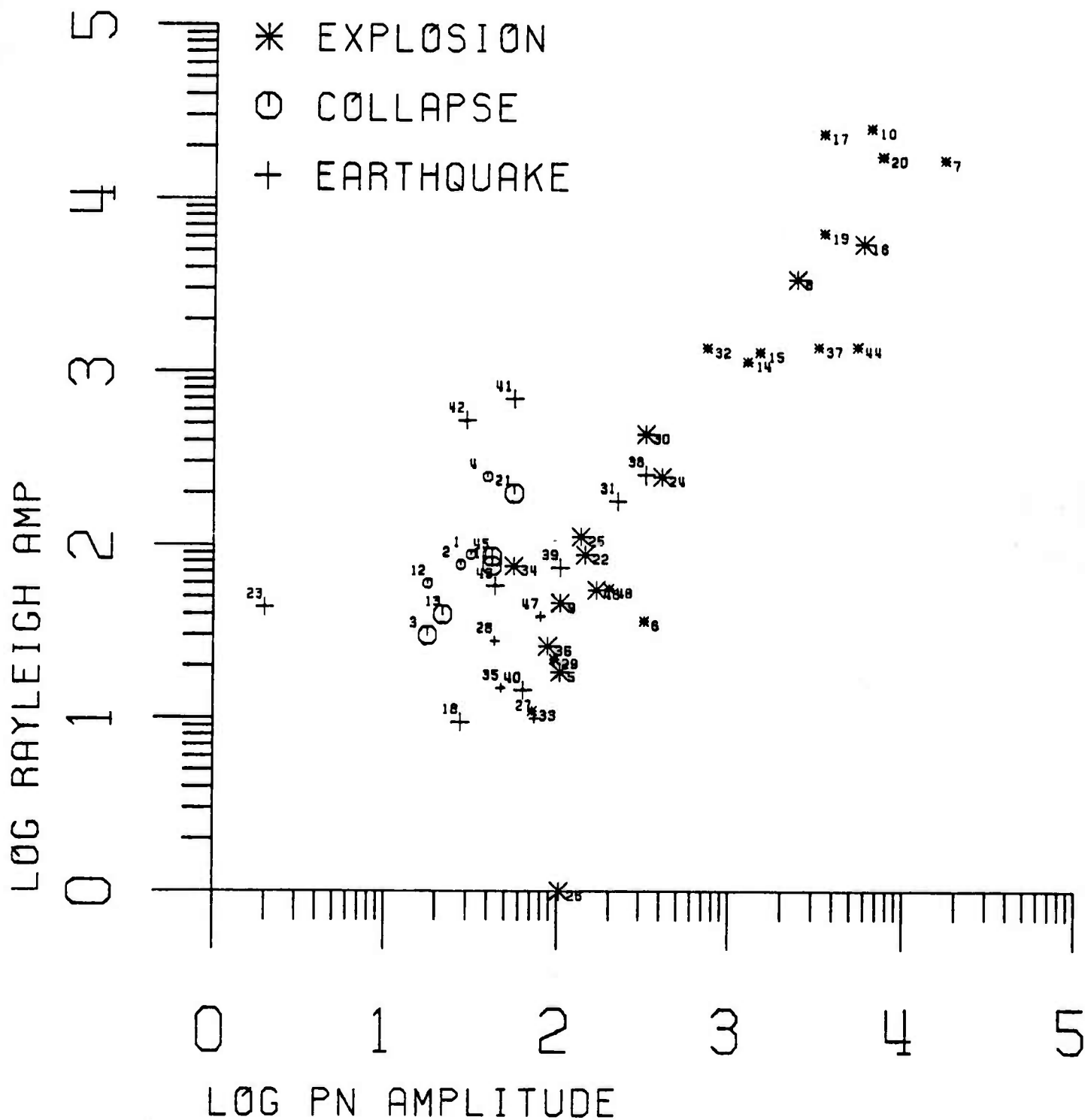


Figure 3.1. Pn versus Rayleigh discrimination for events about 400 km from the Berkeley station Jamestown. Event numbers refer to Table 1.

IDENTIFIER	EVENT NO	PN AMP	RAYLEIGH AMP	COMMENTS
1975 JUN 27 0727	1	32	88*	COLLAPSE
1975 JUN 28 1948	2	28	77*	COLLAPSE
1975 JUL 01 0451	3	18	30	COLLAPSE
1975 JUL 01 1814	4	40	249*	COLLAPSE
1975 SEP 06 1700	5	104	18	EXPLOSION
1975 OCT 24 1712	6	323*	57	EXPLOSION
1975 OCT 28 1430	7	17000*	16800	EXPLOSION
1975 NOV 20 1500	8	2450	3440	EXPLOSION
1975 NOV 26 1530	9	104	47	EXPLOSION
1976 JAN 03 1915	10	6420*	25600	EXPLOSION
1976 JAN 04 0118	11	42	76	COLLAPSE
1976 JAN 04 1616	12	18+	60+	COLLAPSE
1976 JAN 17 2140	13	22	40	COLLAPSE
1976 FEB 04 1420	14	1275*	1160*	EXPLOSION
1976 FEB 04 1440	15	1500	1309*	EXPLOSION
1976 FEB 12 1445	16	5900	5525	EXPLOSION
1976 FEB 14 1130	17	3434*	24000	EXPLOSION
1976 FEB 19 1701	18	28	10	EARTHQUAKE, AZ 130, MAG 4.3, D 332
1976 MAR 09 1400	19	3485*	6400	EXPLOSION
1976 MAR 14 1430	20	7480*	17600	EXPLOSION
1976 MAR 14 1525	21	56	200	COLLAPSE
1976 MAY 12 1950	22	144	88	EXPLOSION
1976 JUN 07 0035	23	2	44	EARTHQUAKE, AZ 115, MAG 4.1, D 392
1976 AUG 26 1430	24	408	248	EXPLOSION
1976 DEC 08 1450	25	136	112	EXPLOSION
1976 DEC 21 1509	26	104	1	EXPLOSION
1977 JAN 13 0719	27	74	10*	EARTHQUAKE, AZ 170, MAG 3.8, D 370
1977 JAN 13 2009	28	44+	28	EARTHQUAKE, AZ 330, MAG 3.7, D 377
1977 FEB 16 1753	29	96	22*	EXPLOSION
1977 AUG 04 1640	30	328	440	EXPLOSION
1977 AUG 12 0220	31	224	180	EARTHQUAKE, AZ 170, MAG 4.8, D 421
1977 AUG 19 1755	32	744	1386*	EXPLOSION
1977 SEP 15 1436	33	72	11*	EXPLOSION
1977 OCT 26 1415	34	56	76	EXPLOSION
1977 NOV 10 0235	35	48+	15	EARTHQUAKE, AZ 125, MAG 4.0, D 302
1977 NOV 17 1930	36	88	26	EXPLOSION
1977 DEC 14 1530	37	3264*	1400	EXPLOSION
1978 FEB 14 0435	38	328	256	EARTHQUAKE, AZ 45, MAG 4.8, D 340
1978 MAY 23 0547	39	104	74	EARTHQUAKE, AZ 20, MAG 4.6, D 434
1978 JUN 16 0421	40	64	15	EARTHQUAKE, AZ 170, MAG 4.3, D 345
1978 AUG 01 0902	41	56	700	EARTHQUAKE, AZ 350, MAG 4.6, D 397
1978 AUG 01 0947	42	30	528	EARTHQUAKE, AZ 350, MAG 4.5, D 397
1978 AUG 01 1026	43	44	58	EARTHQUAKE, AZ 350, MAG 4.2, D 397
1978 AUG 31 1400	44	5440*	1400	EXPLOSION
1978 AUG 31 2356	45	42	86	COLLAPSE
1978 NOV 02 1525	46	168	55	EXPLOSION
1979 JAN 06 0120	47	80+	39	EARTHQUAKE, AZ 75, MAG 4.2, D 377
1979 JAN 24 1800	48	200	56 *	EXPLOSION

* - READINGS BY CONVERSION TO STANDARD ONES (SEE TEXT)

+ - POOR READINGS

Table 1. Basic data taken for the investigation of the Pn versus Rayleigh discriminant. "AZ", "MAG", AND "D" are azimuth from Jamestown to the event, the local magnitude, and distance in km.

$$SPZ = (17.1 \pm 6)BBV \text{ (15 cases),}$$

or

$$SPZ = (34.3 \pm 12)DHG \text{ (8 cases).}$$

The observations starred in Table 1 are those for which adjusted SPZ readings are given (smaller symbols in the figure).

The results confirm my suspicion of many years' standing: the discriminant fails. As a group only hole collapses are separated from the explosions. This highlights the discussion presented in Peppin (1974). We are faced with an empirical method that seems to imply a possible discrimination of earthquakes from explosions; but we are not sure that the discriminant will be effective if applied to a region of interest elsewhere (i.e., the Soviet Union). Only this year have I obtained a means to investigate the theoretical causes for the PN-Rayleigh discriminant (see next section). However, given this negative outcome, the results of that analysis would appear of less interest.

Note that the situation we have presented is really bad for the effectiveness of this discriminant, because all of the stations Berkeley, Jamestown, and Mina are roughly the same azimuth from the test site. The fact that the near and far stations seem to provide effective discrimination and the middle one not is very bad news for him desirous of applying this discriminant to any case of real interest.

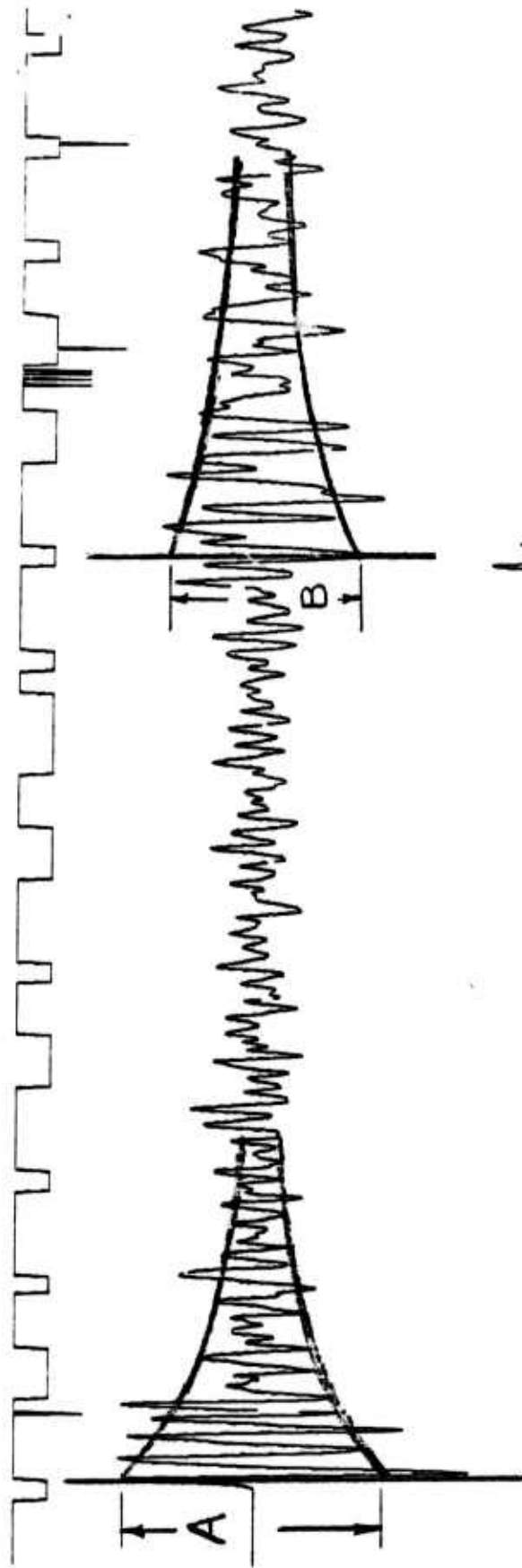
3.2. P versus S Discriminant at Jamestown

In performing the data search for the previous section, I noticed that one could tell at a glance which events were earthquakes and which were not. In virtually all cases the earthquakes had visibly and obviously larger amplitudes of the Sg waves relative to Pg. Various authors have commented on this beginning with the first paper on discrimination (Leet, 1962): since explosions are symmetric sources, they should generate less S energy than a shear source. Indeed, this is taken to be the cause of the Ms:mb discriminant, since both P and S leaving the source generate Rayleigh waves (Douglas et. al., 1971). Murphy and Lahoud (1975) have given a more detailed account of this phenomenon for near-regional records of NTS earthquakes and explosions.

Motivated by the above, I made a comparison of the ratio of Sg to Pg maximum amplitude for a superset of the events used in Section 2.1. The discrimination technique I describe below is simple to apply among its advantages, and I have been able to place quantitative bounds on its range of effectiveness.

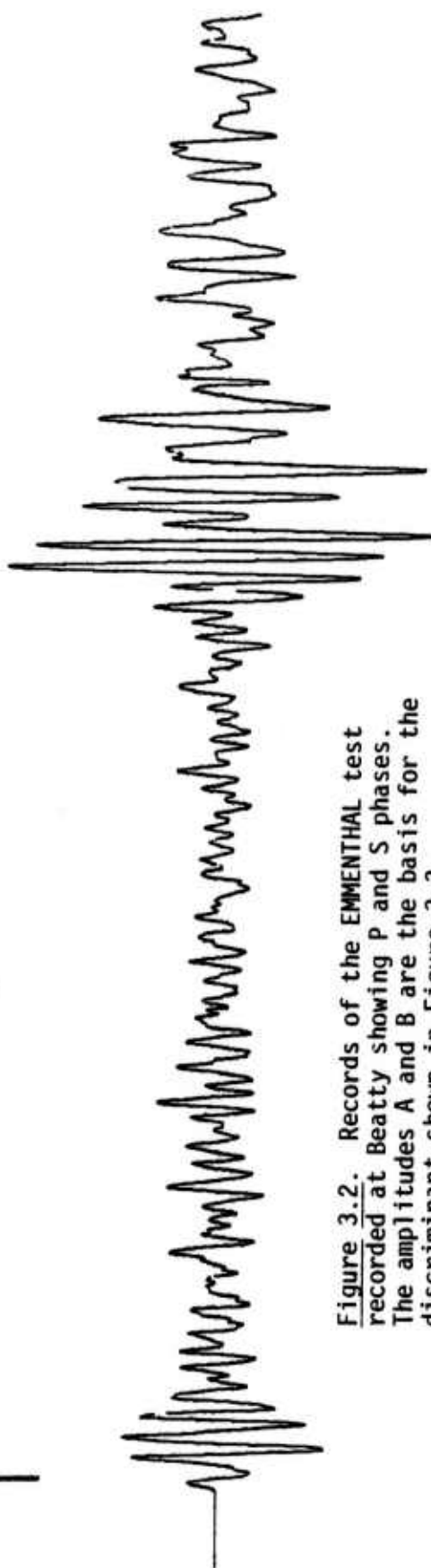
In a study of 60 events I first attempted to see if a spectral estimate would be better than an analog one. However, visually it appeared that discrimination based on wideband spectral power would be less effective than a measurement of maximum amplitude (and indeed Peppin and McEvilly, 1973 had found no luck in their attempts to develop a discriminant on wideband spectral averages of the Pg phase).

The scheme adopted was as follows. First, draw an envelope around the bursts of Pg and Sg energy (Figure 3.2); this is an attempt to smooth the data partially rather than measure the isolated, sharp maximum peaks. Measure the 0-pk height of the envelope at the onset times of the Pg and Sg phases (i.e.,



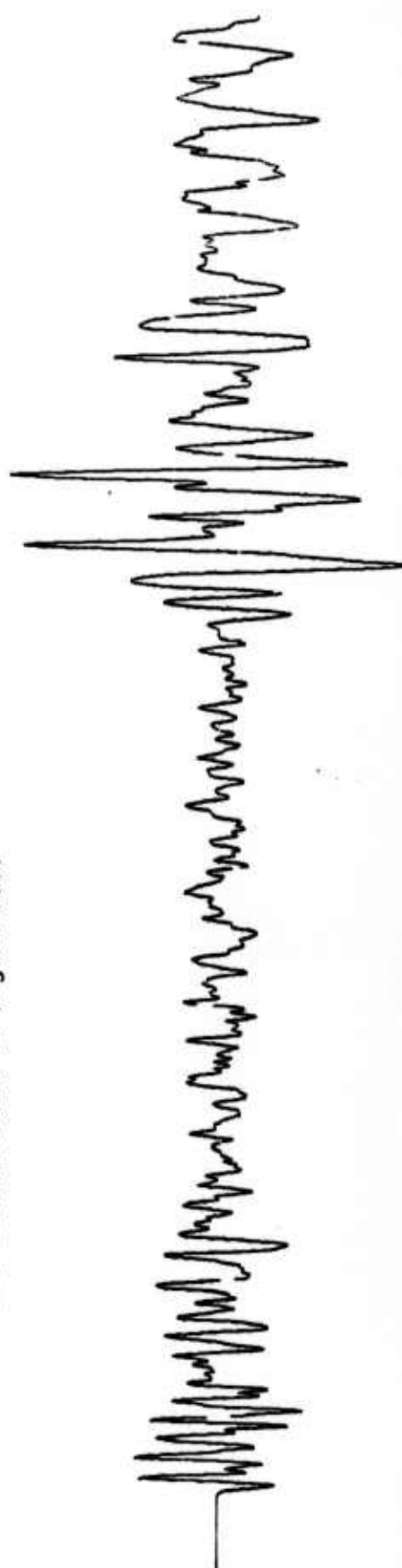
Z

16032.



R

17248.



T

19360.

Figure 3.2. Records of the EMMENTAL test recorded at Beatty showing P and S phases. The amplitudes A and B are the basis for the discriminant shown in Figure 3.3.

BEATTY.DAT

the ratio B to A in the Figure) as seen on the SPZ trace played out on a visicorder. Plot this ratio as a function of local magnitude. We are dealing with a tremendous range of amplitudes, so empirical adjustments are made to connect the different components recorded by the Jamestown system as in the previous section. These adjustments were

SPZ = DHG(17.6 ± 7.8) for P, 23 observations

SPZ = DHG(13.6 ± 6.1) for S, 23 observations

SPZ = BBV(13.9 ± 4.2) for P, 14 observations

SPZ = BBV(13.0 ± 4.5) for S, 24 observations

Results of the analysis are given in Table 2 and Figure 3.3. Note that the explosions separate well from the natural earthquakes, but that the hole collapses extend far up into the earthquake population. All explosions show an S to P ratio less than 2 and all earthquakes except one (28 in Table 2) show a ratio as least as great as 2.

In order to assign statistical significance to the degree of separation, I computed an uncertainty for those events recorded on each of BBZ, DHG, or SPZ. These uncertainties are shown in Figure 3.4. I have displaced these 95% error bars left or right of the event in question for visual clarity of presentation. Standard errors amount to 32%, 17%, and 15% of the mean for collapses, explosions, and earthquakes, respectively, where we have ignored the earthquake with huge error bars at Shasta that is obviously not an explosion from the appearance of the records taken. In Figures 3.3 and 3.4 we have drawn a horizontal line separating the populations at a ratio of 2 and 95% error bars 20% of the mean

around either side of it. Of sixty events ranging in magnitude from 3.5 to 6.5 13 are definitely identified as not explosions, 36 are definitely identified as explosions, and the remaining 11 are unresolved. A single earthquake (28 in Table 2 and Figure 3.4) falls into the explosion population. However, this event (23 in Table 1 and Figure 3.1) is definitely identified as an earthquake by the PN-Rayleigh discriminant. For discrimination purposes, it is not a fatal flaw that many collapses are misidentified as explosions, since the presence of a collapse implies (with about 99% probability) an explosion within the last week. Many of the collapses can be identified by their large surface wave excitation (Figure 3.1), and spectral ratio techniques could identify many more (most collapses show obviously longer periods in their Pg waves than are seen in explosions of comparable magnitude: see the work of Stump, 1979 for example).

3.3. Seismic Discrimination at Jamestown: Summary

If we use as a primary discriminant the S/P ratio method described in Section 3.2 and The PN-Rayleigh discriminant as a secondary one, 28 of 30 explosions are identified with certainty; no earthquake in a region extending from northern California, through Nevada, and back into southern California is identified as an explosion. Hole collapses remain ambiguously or incorrectly identified, but the identification of these should be no problem. The S/P ratio method has some compelling and obvious advantages: (1) it is effective to magnitudes as small as can be seen on high-gain, short-period seismographs at near-regional distances, i.e., local magnitude 3.0 or less; (2) it is simple to apply; (3) it is reasonably easy to understand how it works; (4) plots like Figure 3.3 can be carried over to another region without change as a ratio is

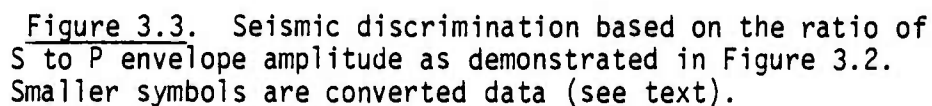


Figure 3.3. Seismic discrimination based on the ratio of S to P envelope amplitude as demonstrated in Figure 3.2. Smaller symbols are converted data (see text).

IDENTIFIER	EVENT NO	P AMP	S TO P RATIO	COMMENTS
1975 JUN 27 0727	1	15.	1.12*	COLLAPSE
1975 JUN 28 0948	2	14.	1.10*	COLLAPSE
1975 JUL 01 0451	3	12.	1.05	COLLAPSE
1975 JUL 01 1814	4	39.	2.68	COLLAPSE
1975 SEP 06 1700	5	22.	1.11	EXPLOSION
1975 OCT 24 1712	6	67.	1.24	EXPLOSION
1975 OCT 28 1430	7	76.	0.32	EXPLOSION
1975 NOV 18 1530	8	12.	1.75	EXPLOSION
1975 NOV 20 1500	9	1400.	0.50	EXPLOSION
1975 NOV 26 1530	10	36.	1.47	EXPLOSION
1976 JAN 03 1915	11	4200.	0.48	EXPLOSION
1976 JAN 04 0118	12	13.	1.26	COLLAPSE
1976 JAN 04 1616	13	8.	2.40	COLLAPSE
1976 JAN 18 0720	14	14.	1.75	COLLAPSE
1976 JAN 21 1840	15	9.	2.11	COLLAPSE
1976 FEB 03 0015	16	8.	1.33	COLLAPSE
1976 FEB 04 1420	17	480.	1.20	EXPLOSION
1976 FEB 04 1440	18	416.	1.58	EXPLOSION
1976 FEB 12 1445	19	1400.	0.71	EXPLOSION
1976 FEB 14 1130	20	3800.	0.53	EXPLOSION
1976 FEB 19 1701	21	15.	3.97	EARTHQUAKE, AZ 130, MAG 4.3, D 332
1976 FEB 26 1450	22	8.	1.20	EXPLOSION
1976 MAR 09 1400	23	2000.	1.33	EXPLOSION
1976 MAR 09 1655	24	16.	1.26	COLLAPSE
1976 MAR 14 1450	25	4400.	0.45	EXPLOSION
1976 MAR 14 1525	26	30.	1.22*	COLLAPSE
1976 MAY 12 1950	27	53.	1.18	EXPLOSION
1976 JUN 07 0035	28	13.	1.77	EARTHQUAKE, AZ 115, MAG 4.1, D 392
1976 JUN 19 1025	29	7.	1.71	EXPLOSION
1976 AUG 22 1014	30	6.	2.26	EARTHQUAKE, AZ 45, MAG 4.0, D 340
1976 AUG 26 1430	31	140.	1.47	EXPLOSION
1976 DEC 08 1450	32	69.	1.12	EXPLOSION
1976 DEC 21 1509	33	31.	0.98	EXPLOSION
1977 JAN 13 0709	34	13.	2.00*	EARTHQUAKE, AZ 170, MAG 3.8, D 370
1977 JAN 13 2009	35	6.	3.96	EARTHQUAKE, AZ 330, MAG 3.7, D 377
1977 FEB 16 1753	36	25.	1.25	EXPLOSION
1977 MAY 31 1640	37	3.	3.67	EARTHQUAKE, AZ 330, MAG 3.7, D 330
1977 AUG 04 1640	38	130.	0.86*	EXPLOSION
1977 AUG 12 0220	39	40.	3.73	EARTHQUAKE, AZ 170, MAG 4.8, D 421
1977 AUG 19 1755	40	471.	1.27*	EXPLOSION
1977 SEP 15 1436	41	18.	1.28	EXPLOSION
1977 OCT 26 1415	42	31.	1.54	EXPLOSION
1977 NOV 10 0235	43	14.	3.28	EARTHQUAKE, AZ 125, MAG 4.0, D 302
1977 NOV 17 1930	44	40.	1.18	EXPLOSION
1977 DEC 14 1530	45	496.	1.13	EXPLOSION
1978 FEB 14 0435	46	16.	2.96	EARTHQUAKE, AZ 45, MAG 4.8, D 340
1978 MAY 23 0547	47	20.	4.45	EARTHQUAKE, AZ 20, MAG 4.6, D 434
1978 JUN 16 0421	48	64.	2.17	EARTHQUAKE, AZ 170, MAG 4.3, D 345
1978 JUL 07 1400	49	24.	1.16*	EXPLOSION
1978 JUL 29 2232	50	52.	2.08	EARTHQUAKE, AZ 45, MAG 4.0, D 340
1978 AUG 01 0902	51	40.	3.87	EARTHQUAKE, AZ 350, MAG 4.6, D 397
1978 AUG 01 0947	52	24.	5.27	EARTHQUAKE, AZ 350, MAG 4.5, D 397
1978 AUG 01 1026	53	16.	2.21	EARTHQUAKE, AZ 350, MAG 4.2, D 397
1978 AUG 31 1400	54	1500.	0.67	EXPLOSION
1978 AUG 31 2356	55	21.	0.50	COLLAPSE
1978 NOV 02 1525	56	32.	0.71	EXPLOSION
1979 JAN 06 0120	57	16.	2.55	EARTHQUAKE, AZ 75, MAG 4.2, D 377
1979 JAN 24 1800	58	25.	1.39	EXPLOSION
1979 FEB 22 0716	59	8.	4.16	EARTHQUAKE, AZ 0, MAG 3.5, D 230
1979 FEB 22 1557	60	700.	2.54	EARTHQUAKE, AZ 0, MAG 5.0, D 230

* -BY CONVERSION TO JAMESTOWN SHORT PERIOD (SEE TEXT)

Table 2. Same format as Table 1 for the S/P discrimination.

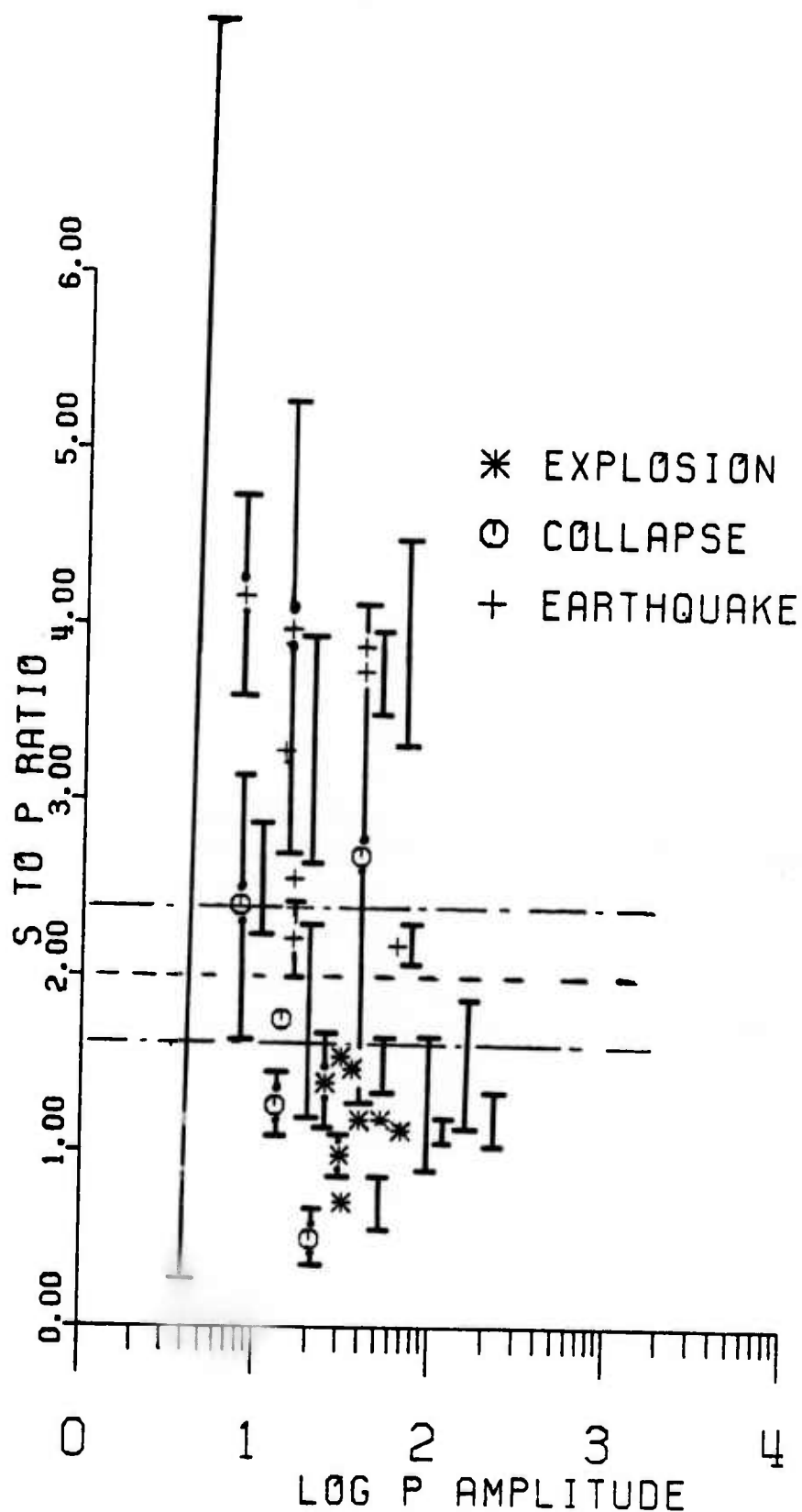


Figure 3.4. This figure used to estimate the significance of the data presented in Figure 3.3. Where three readings of the ratio of S to P amplitude were available, a standard deviation was computed and plotted here. The horizontal lines delimit the decision band: earthquakes are above it and explosions below.

measured, while in Figure 3.1 we are required to calibrate the plot for each region (which is impossible in the regions of interest); (5) the phases measured, i.e., P_g and S_g (or " L_g " in the parlance of Russian and Midwestern American seismologists) will have envelope amplitudes not strongly dependent on source focal mechanism as they are crustal channel waves that sample the focal sphere at many takeoff angles. The simple explanation of why the discriminant works is in the energy leaving the source (hence available to travel outward as P_g or S_g): shear sources send out far more (factor of ten) energy in S than in P . This is the same reason given for the efficiency of the $M_s:m_b$ discriminant as noted above.

It is worth noting that the data discussed in this section raises serious questions as to whether we understand in even a fundamental way the nature of surface-wave excitation by explosions. Although it is claimed by some that the S leaving the source excites the bulk of the surface waves leaving a seismic source (hence the $M_s:m_b$ discriminant), I saw many explosions with essentially no S_g phase that generated huge surface waves (hence failure of the discriminant in Figure 3.1). That is, the S_g phase seen in explosions appears uncorrelated with the amplitude of the surface waves. I believe that the mechanism of surface wave excitation from explosions departs significantly from processes which can be described by first-order or linear theory (which encompasses almost the totality of the work done at near-regional distances in seismology). As I have looked at more of this data, I become more and more convinced that Viecelli's (1973) treatment of the generation of these waves through the mechanism of spall closure is a better route toward understanding this phenomenon. A similar argument may apply also to the generation of body waves, but the modelling done so far seems more self-consistent to me than the work on surface waves. Because of

these feelings, I would recommend stronger emphasis on discrimination methods which utilize body waves, as I believe that such methods are more likely to be capable of realistic theoretical treatment.

Finally, I would like to qualify what may appear to be an enthusiastic endorsement of the S/P method of discrimination discussed above. First, the populations do not separate by any very large margin, so failures of the discriminant are bound to occur in other areas where the populations move slightly closer together. Second, the failure to discriminate Event 28 in Table 2 is particularly disturbing, as it was the natural earthquake closest of any studied here to the test site. Bakun and Johnson (1970) had found a dandy discriminant that turned out to fail for events on the test site (i.e., the Massachusetts Mountain earthquakes were identified as explosions by their method: unpublished data, 1973) as were those aftershocks of nuclear explosions that were not collapses. Of note is that Murphy and Lahoud (1975), using a rather more sophisticated procedure based on the ratio of S to P, clearly discriminated the Massachusetts Mountain mainshock at regional distances (their plots show an S to P ratio of 4 or more). It is probable that refinements along the lines presented by these authors would lead to a significantly more robust discriminant.

As a final note of pessimism, note in Figure 3.3 that the S/P ratio seems to be converging at the small magnitude end of the plot, precisely the area of greatest interest.

4. SEISMIC DISCRIMINATION AT REGIONAL DISTANCES USING PN

In this section I describe work aimed at obtaining a seismic discriminant

based on analysis of the PN phase alone. The study is motivated by some theoretical and practical considerations. First, PN leaves the source at rather steep angles of incidence; thus we sample a rather confined area of the focal sphere, which has the potential for increasing the precision of the determination relative to measurement of, say, the Pg phase. Second, PN travels deep in the crust, thus (perhaps) avoiding some of the upper-crust complexities that are sure to hinder detailed understanding of the Pg phase. For the purpose of routine identification and discrimination, the PN phase is an attractive one to consider and, so far as I know, such a study has not previously been attempted.

The method to be used is inversion for the seismic moment tensor as described in previous sections. To this end we have selected two low-yield events on the test site, one (12 May 1976 at 1950 GCT) on Yucca Flat and the other (02 Nov 1978, 1626 GCT) on Pahute Mesa. Data from the Lawrence Livermore Laboratory fast tapes was digitized at 250 samples per second and decimated to 50 samples/sec after digital alias filtering at 10 Hz. Three-component data at Mina, Kanab, Landers, and Elko, distributed around the test site in azimuths at distances of 200 to 400 km, was obtained. This data provides an ideal proving ground for discriminants of this kind, as the data quality is excellent.

The discriminant I intend to test is based on the prediction of ground motion from the canonical sources required for input to Brian Stump's inversion code (Stump and Johnson, 1977). Accordingly, Green's functions were prepared using MEXEC for a model similar to that presented by Priestley and Brune (1978) based on Great Basin surface wave analysis, i.e., a 3-layer crust over a mantle with a PN velocity of 7.8 km/sec. Due to anisotropy or some other failure of the Priestley and Brune model at a precision of tenths of a second, predicted

onset times of PN were inconsistent at the four stations. Therefore, I adjusted the times so that the onset times of the theoretical and observed data agreed to avoid spurious offsets in phase that would be returned by moment tensor inversion.

It is clear that the present exercise is going to be a severe test of the moment tensor method. Consider, for example, Figures 4.1 and 4.2. In this and other figures, groups of four traces are shown. The top trace is theoretical ground motion at the appropriate receiver site for a step function source. The next trace is the result of passing the theoretical trace through the instrument (velocity flat systems in this case). The third trace shows the effect of inserting a finite source time, and should be compared with the fourth trace, the observations. In Figures 4.1 and 4.2 we compare vertical components for the 02 November explosion as recorded at Mina and Kanab (left and right images of Figure 4.1) and Landers and Elko (left and right images of Figure 4.2). Note in Figure 4.1 that the theoretical trace shown includes a part of P_g , so that P_n is not clearly seen. The steppy synthetic ground motions on the other three stations are what is expected by the theory (P_n at distance mirrors motion at the source). Note that the theoretical P_n waveforms are all similar, but the data at the four stations are quite different. Note also the significant difference in frequency content. Theoretical source rise times of 0.4 second and overshoot ratios of about 1.5 to 1 were included in the convolution for source finiteness (third traces of each image). Numbers given to the right of each trace indicate maximum trace amplitudes (the bottom trace is scaled to ground velocity in cgs units): note the variations in these from station to station (bottom traces). For generalized ray theory to fit these observations, a crustal model with considerably finer detail will have to be employed.

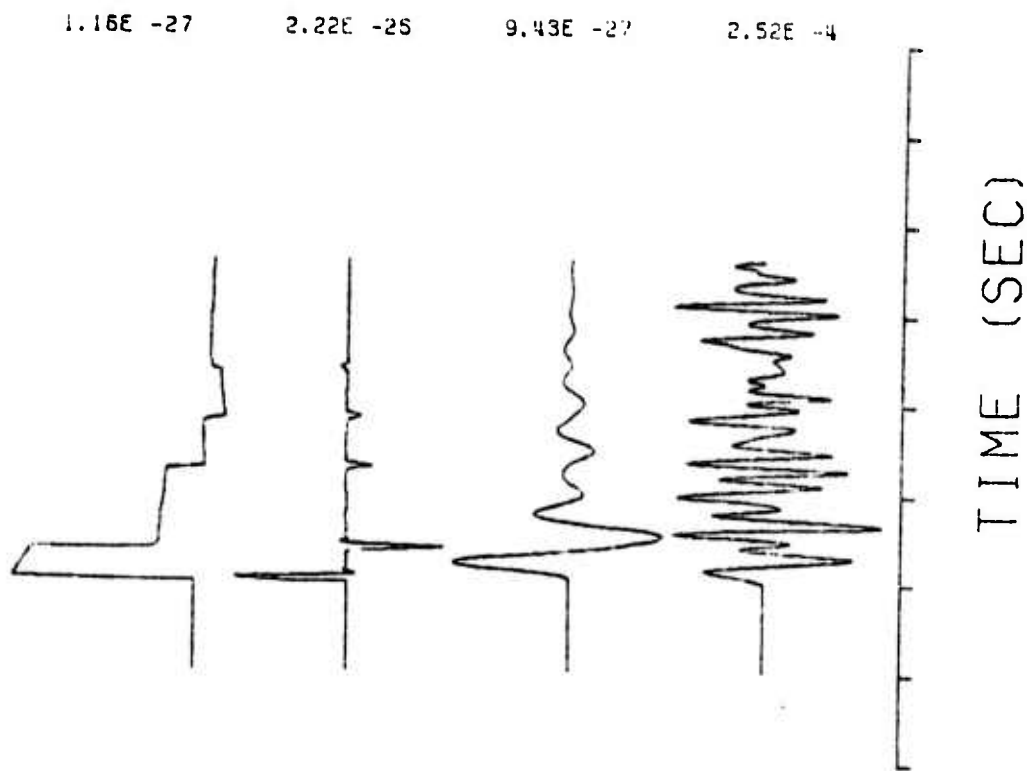
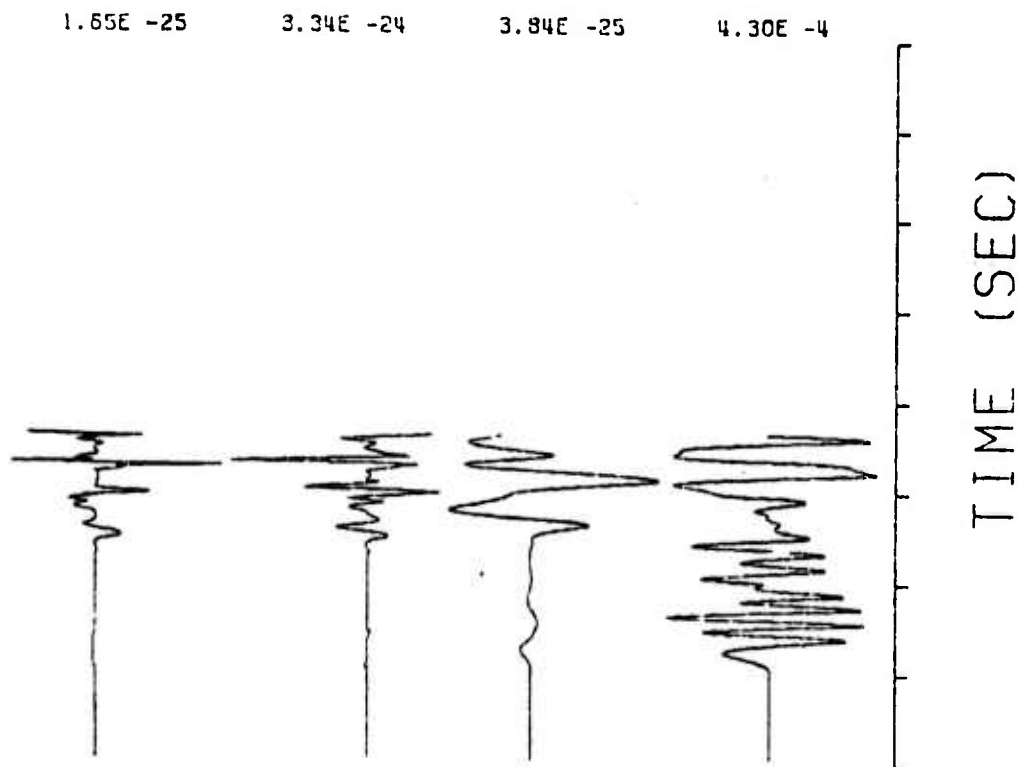


Figure 4.1. Comparison of theoretical versus observed ground motion for the EMMENTHAL test, 02 Nov 1978 at 1525 GCT, Mina left and Kanab right. Top traces: computed ground motion at the respective stations computed by MEXEC; second trace: after passing the first trace through the instrument; third trace: after convolution with a source with 0.4 second rise time and overshoot of 1.5 to 1. All here for the vertical component of the explosion. Observation distance at Mina and Kanab is 205 and 303 km, respectively.

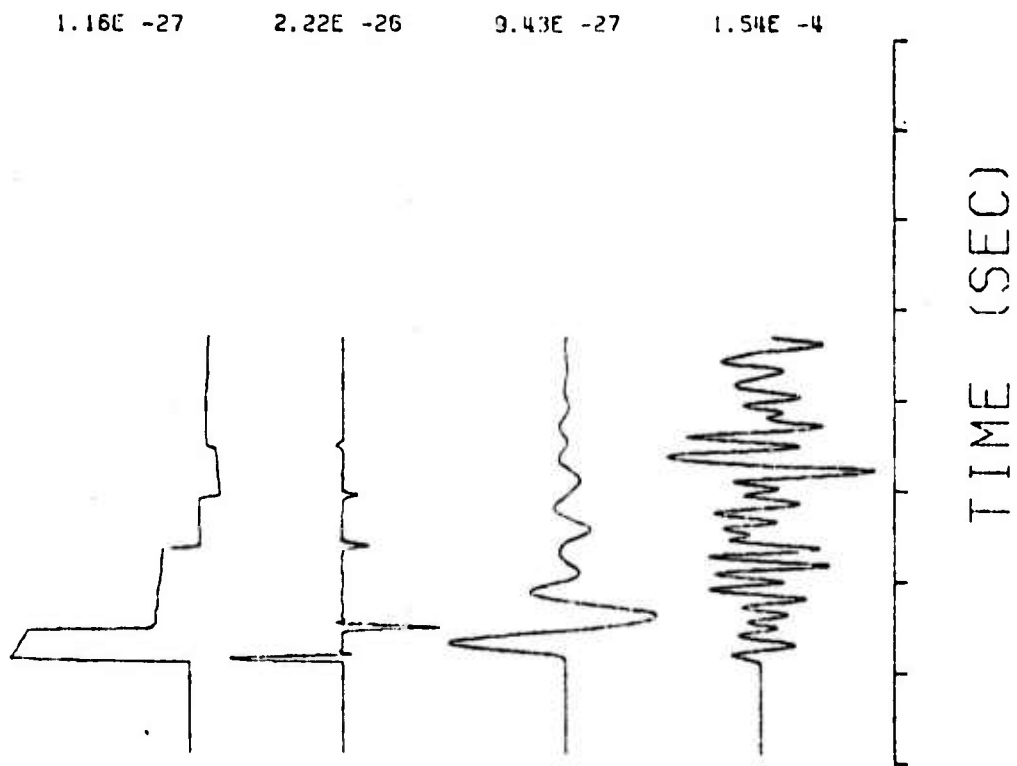
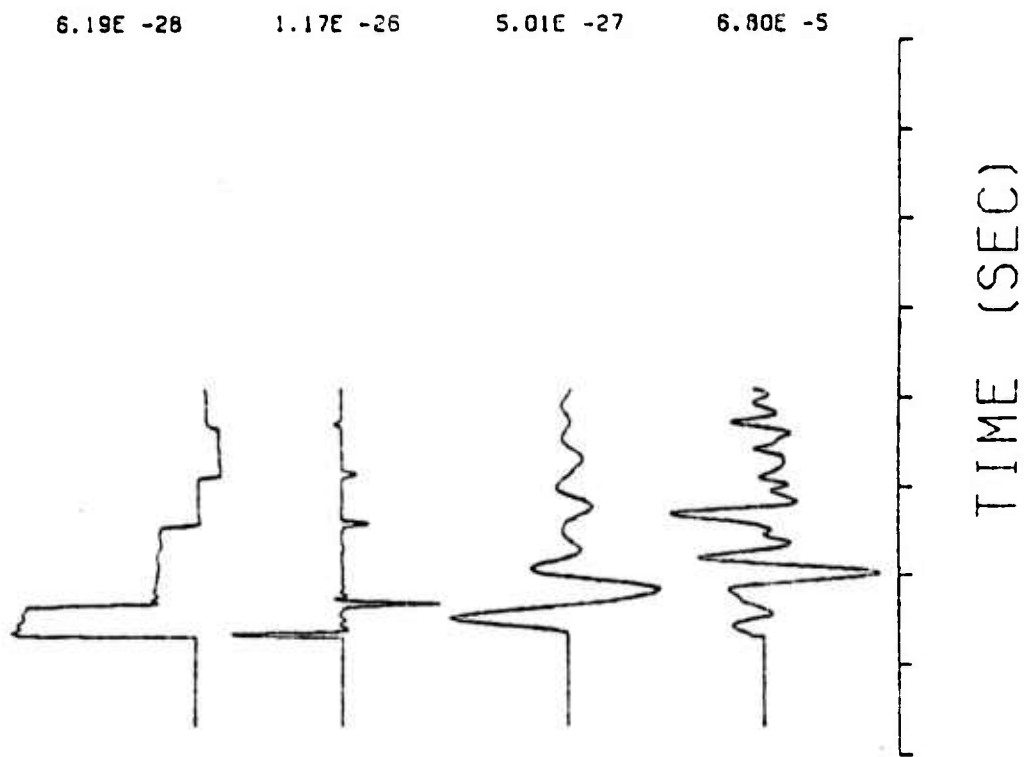


Figure 4.2. Same format as Figure 4.1, but for the vertical components at Landers (left) and Elko (right). Numbers right of each trace are maximum trace amplitude. The data traces are in units of velocity (cm/sec).

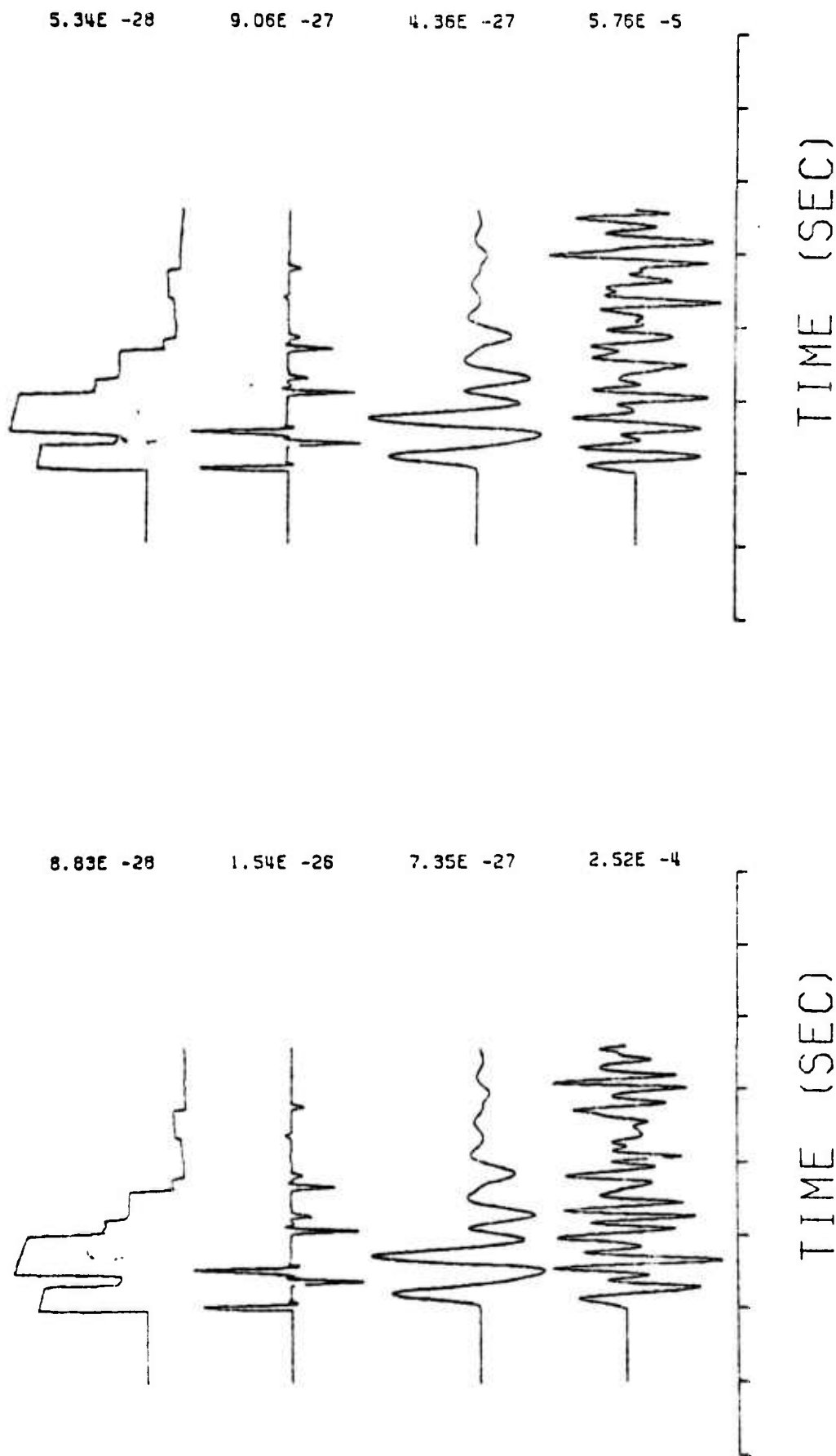


Figure 4.3. This and remaining figures of this section are in the same format, vertical components on the left and radial components on the right. Traces from top to bottom are as in Figures 4.1 and 4.2, i.e., theoretical traces on top and the data on the bottom. Shown for the Landers station are the data and the theoretical displacements to be expected from a strikeslip earthquake oriented 45 degrees off the line from station to epicenter.

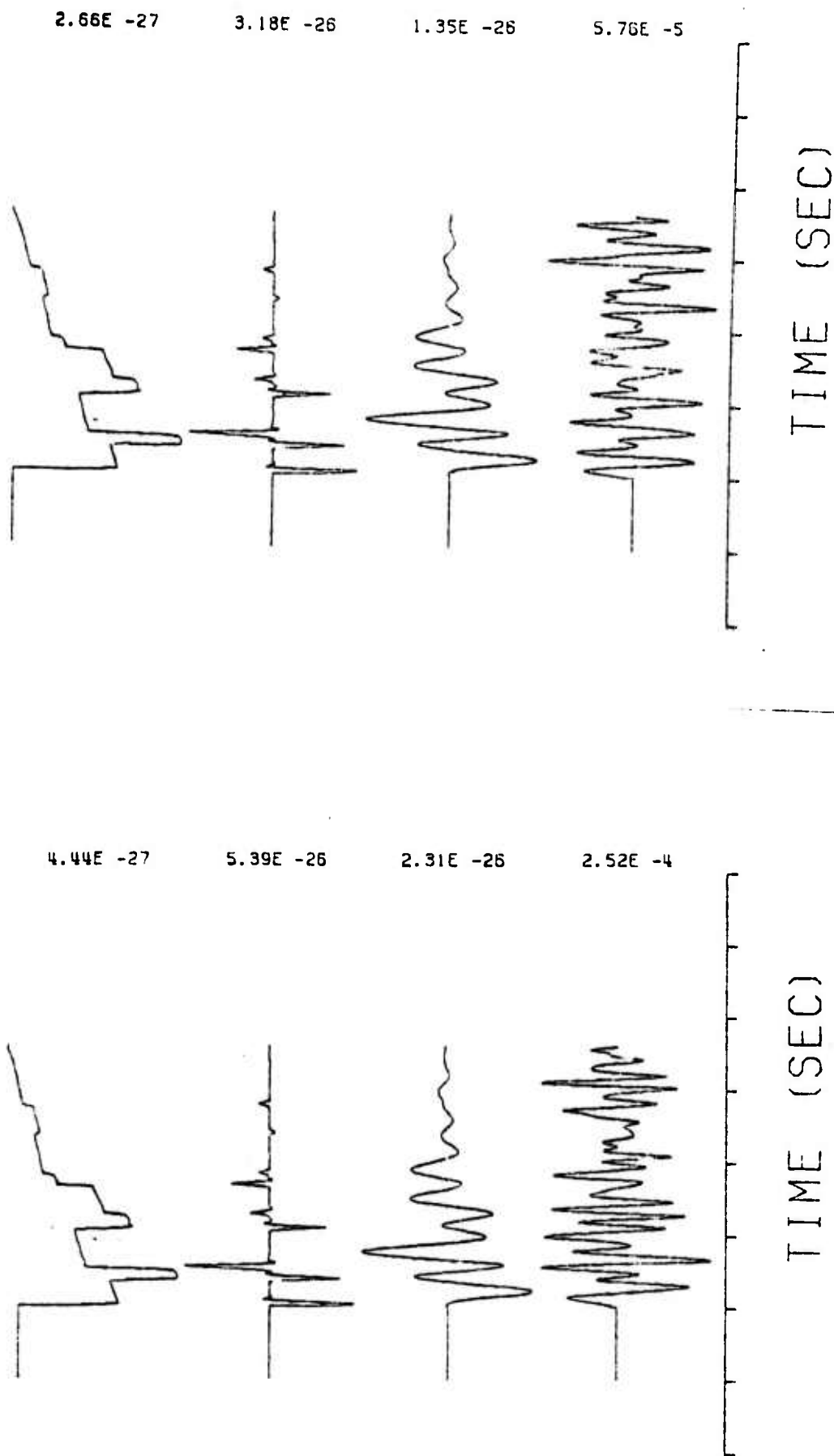


Figure 4.4. Same as Figure 4.3, but for the radial and vertical components of a dip-slip earthquake with fault plane oriented perpendicular to the line from the station to epicenter. Landers station.

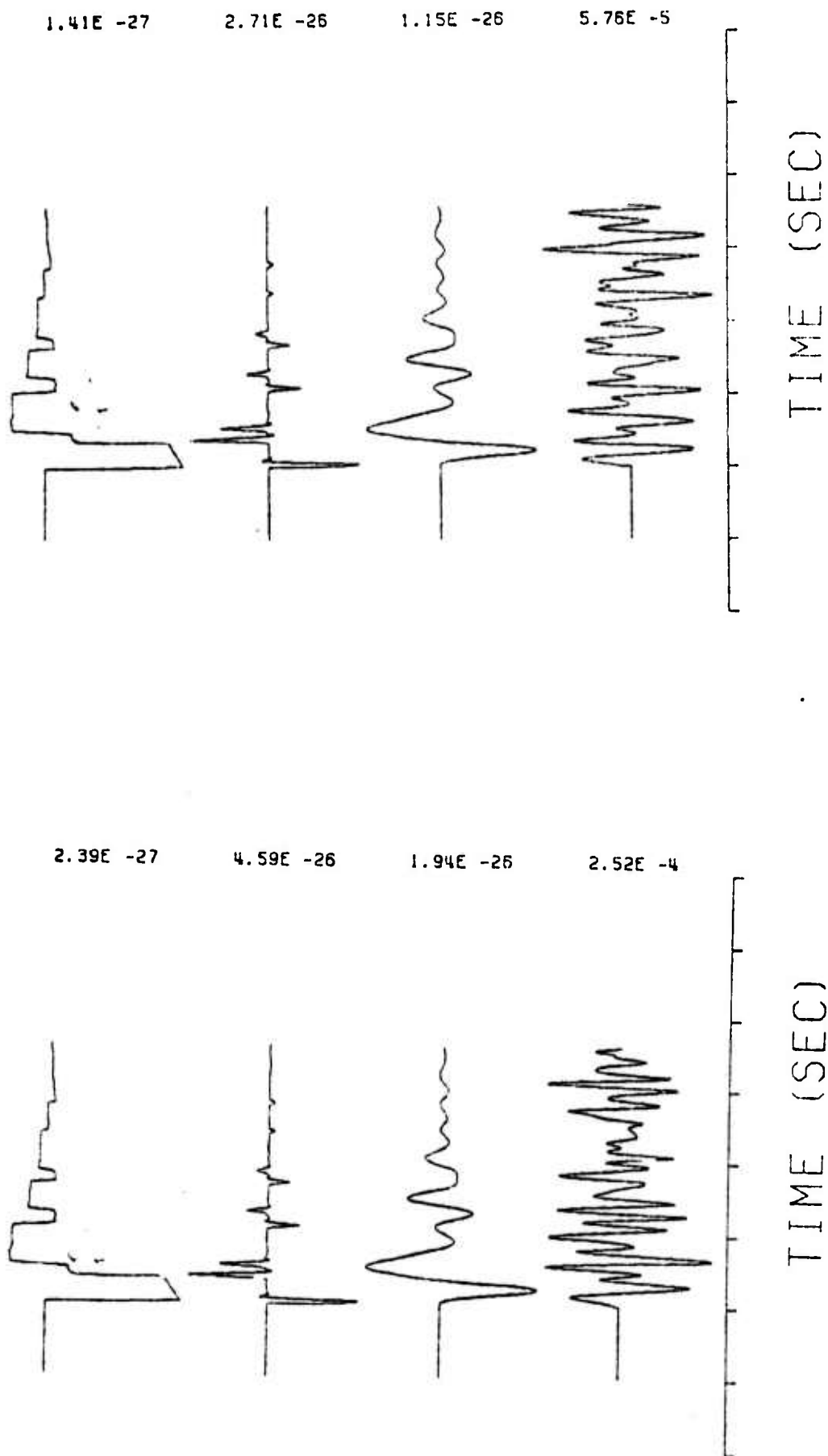


Figure 4.5. Same format as Figure 4.3, again at Landers, but for a source consisting of a compensated linear vector dipole, i.e., $g_{11,1} + g_{12,2} - 2g_{13,3}$.

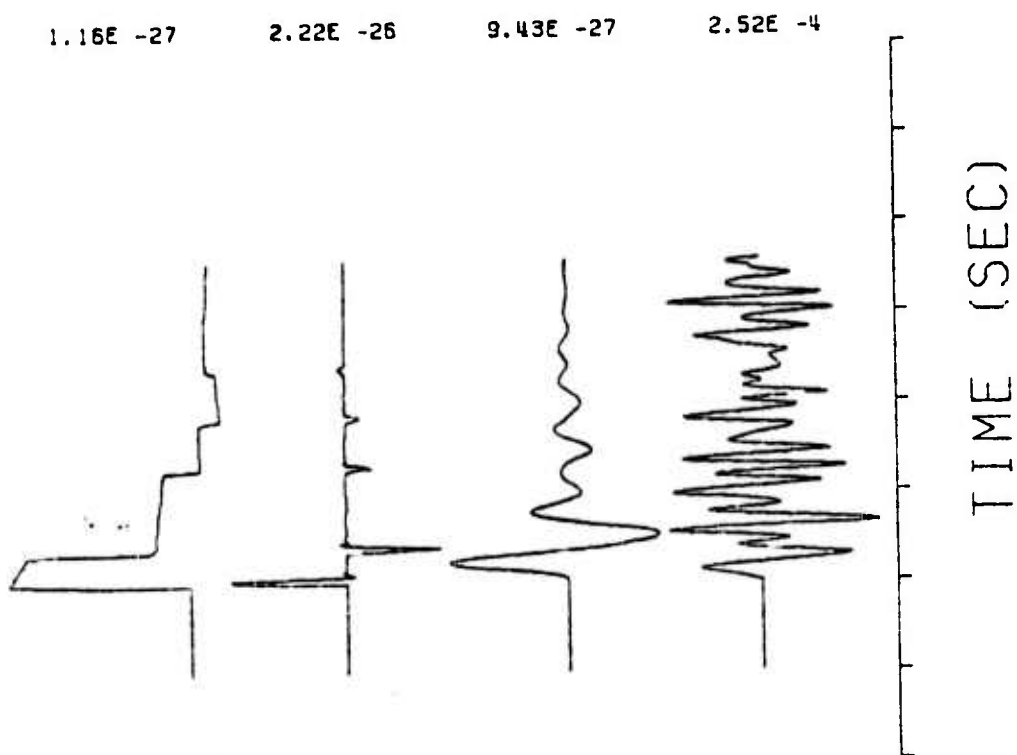
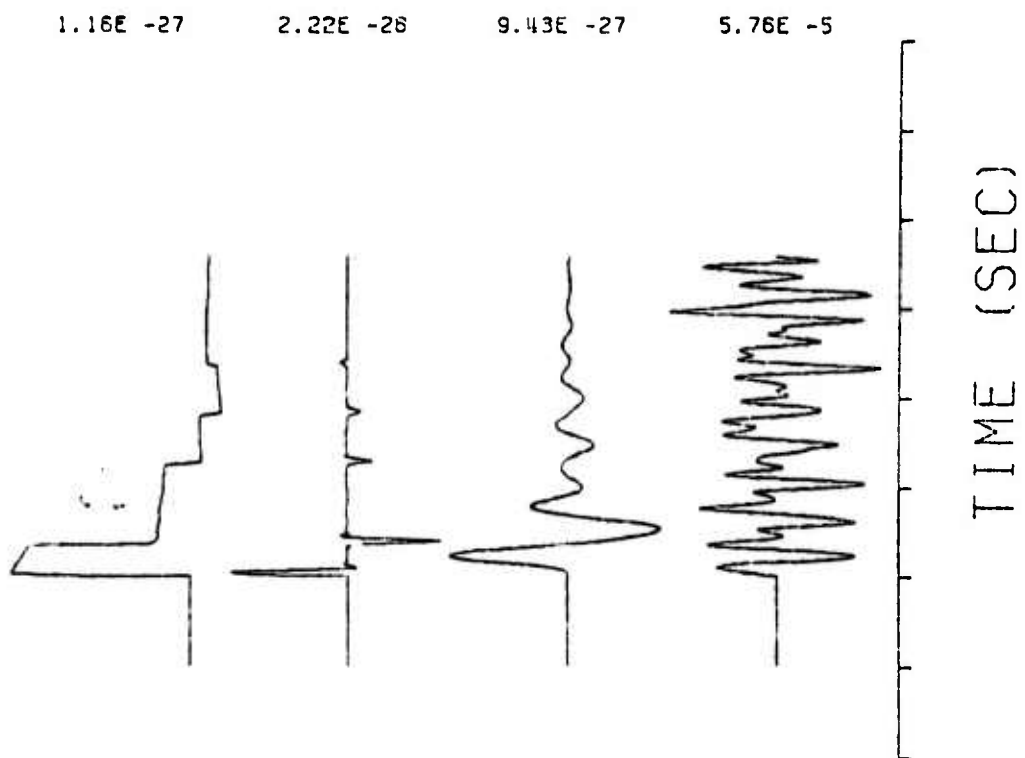


Figure 4.6. Same format as Figure 4.3, but for an explosion source at Landers

In the set of figures 4.3 to 4.6, we compare the appearance of the PN phase produced by explosion and earthquake sources at Landers for the 02 November explosion. In each figure we present the vertical component on the left and the radial component on the right. Figure 4.2 is for a strikeslip earthquake oriented at 45 degrees from the receiver. Figure 4.3 is for a dipslip earthquake whose fault plane is oriented in line with the receiver. Figure 4.4 is the motion from a compensated linear vector dipole. Finally, Figure 4.5 is for the explosion source. Note that the theoretical records for earthquake sources are considerably more complex than those for the explosion, mainly because the latter includes no generalized raypaths that leave the source as an SV wave. However, on all these sources the motions in the PN phase observed lasts considerably longer than the theoretical calculation indicates, and none of them looks particularly like the data.

All of the data and Green's functions shown in this section have been placed on the Cyber 176 computer at Kirtland Air Force Base in Albuquerque, and await the running of Brian Stump's code. In a subsequent report the outcome of this and any follow-on experiments will be described.

5. ANALYSIS OF CLOSE-IN ACCELEROMETER RECORDS OF MEGATON EXPLOSIONS

Peppin (1977), Stump (1979), and Helmberger and Hadley (1980) have presented analyses of close-in (8 km) records of the megaton explosions JORUM and HANDLEY, which occurred, respectively on 16 Sep 1969 at 1430 GCT and 23 Mar 1970 at 1900 GCT. These analyses have grown ever more sophisticated. Peppin's solution is the simplest. That of Stump provides the best fit of theory with data; Helmberger and Hadley have provided the most realistic Green's functions.

Results of these studies are in significant disagreement. While the latter study concludes that overshoot at the source is necessary to fit the observations, the former two do not. The problem is well worth investigating, because this overshoot is relevant to the understanding of body-wave excitation by explosions. In this section I describe efforts aimed at merging the calculations of realistic Green's functions using the MEXEC code with the powerful moment tensor inversion method implemented by Stump. Material in this section is presented at the American Geophysical Union meetings in San Francisco (Peppin, 1979).

In Section 1 I described the development of the MEXEC code. This code permits the determination of multilayer Green's functions at any distance range (although this is not possible as a practical matter for reasons of numerical stability and cost in a wide variety of interesting problems). It was specifically written for the problem described in this section. We have computed four test cases: source in a layer, source below the layer, Helmberger-Hadley model, and extended Helmberger-Hadley model. These are discussed in subsequent subsections.

5.1. Source in a Layer

In Figure 5.1 we summarize the layer models used in the various test cases. For this section, we take the model in the left-center part of the figure, with the original halfspace model used by Peppin (1977) above for comparison. Model parameters are arbitrarily chosen so that the onset time is as observed on the test site, and with Poisson's ratio $1/4$. In Figure 5.2 we show the comparison of the data with the Green's function computed, which contains all first-order

LAYER MODELS

$$\begin{array}{c} \text{surface} \\ \hline \alpha = 3.30 \quad \beta = 1.95 \\ \rho = 2.70 \quad h = 1.3 \end{array} *$$

$$\begin{array}{c} \text{surface} \quad \downarrow \\ \hline \alpha = 3.30 \quad \beta = 1.95 \\ \rho = 2.60 \quad h = 1.3 \end{array} \quad 2 \text{ km} \quad \begin{array}{c} \text{surface} \\ \hline \alpha = 2.00 \quad \beta = 1.20 \quad \rho = 2.50 \quad h = 1.3 \quad \downarrow .65 \\ \alpha = 3.82 \quad \beta = 2.21 \\ \rho = 2.67 \quad h = 1.3 \end{array} *$$

$$\begin{array}{c} \hline \alpha = 6.10 \quad \beta = 3.55 \\ \rho = 2.70 \quad h = 1.3 \end{array} \quad \uparrow$$

$$\begin{array}{c} \text{surface} \quad \downarrow \\ \hline \alpha = 2.70 \quad \beta = 0.8 \quad \rho = 2.60 \quad h = 1.3 \quad .58 \text{ km} \\ \uparrow \quad \alpha = 3.40 \quad \beta = 1.20 \quad \rho = 2.70 \quad .68 \text{ km} \\ \alpha = 3.80 \quad \beta = 1.80 \quad \rho = 2.80 \quad 1.2 \text{ km} \end{array} *$$

$$\begin{array}{c} \hline \alpha = 4.40 \quad \beta = 2.50 \quad \rho = 2.82 \end{array} \quad \uparrow$$

Figure 5.1. Layer models considered in this section drawn with layer thicknesses to scale. Stars represent source. Top model: halfspace case considered by Peppin ([977]); other models: as discussed in the text. Triangles show locations of extended Helmberger-Hadley model.

reflections in the layer including the free-surface reflection. As in the previous section, vertical data is shown on the left, radial on the right. The top trace is theoretical response to a step function; the second trace results from passing the first trace through the accelerometer; the third trace shows the effects of a finite source duration; the fourth trace is data taken on the test site.

Note that a rise time of 0.6 second has been used in Figure 5.2, and an overshoot ratio of 1.05 to 1 (almost no overshoot). If more overshoot is added the fit to the first second of the data is degraded (Figure 5.3). Although the fit on the waveforms of the P onset is pretty good, the relative ratios predicted fail to match the observed by a large factor (note how the theoretical radial is larger, but the observed vertical data is larger: numbers right of each trace in these figures). Thus, although overshoot at the source is evidently not necessary here, the ratio of vertical to radial motion provides a serious problem, the same one discussed by Peppin (1977).

5.2. Source Below a Single Layer

In Figure 5.4 we have placed the source below a slow layer: see the layer model center right in Figure 5.1. Layer parameters are chosen so that: (1) the P onset times agree with the observed, (2) the vertical component of P in the synthetics has about the correct amplitude relative to the radial, and (3) Poisson's ratio is 1/4. The Green's functions include all directs and first-order multiples (with conversions) in the top layer. Note the radial component in Figure 5.4. The theoretical trace fits the data as well as any in this section right through the Rayleigh wave arrival in character, and in fair detail near

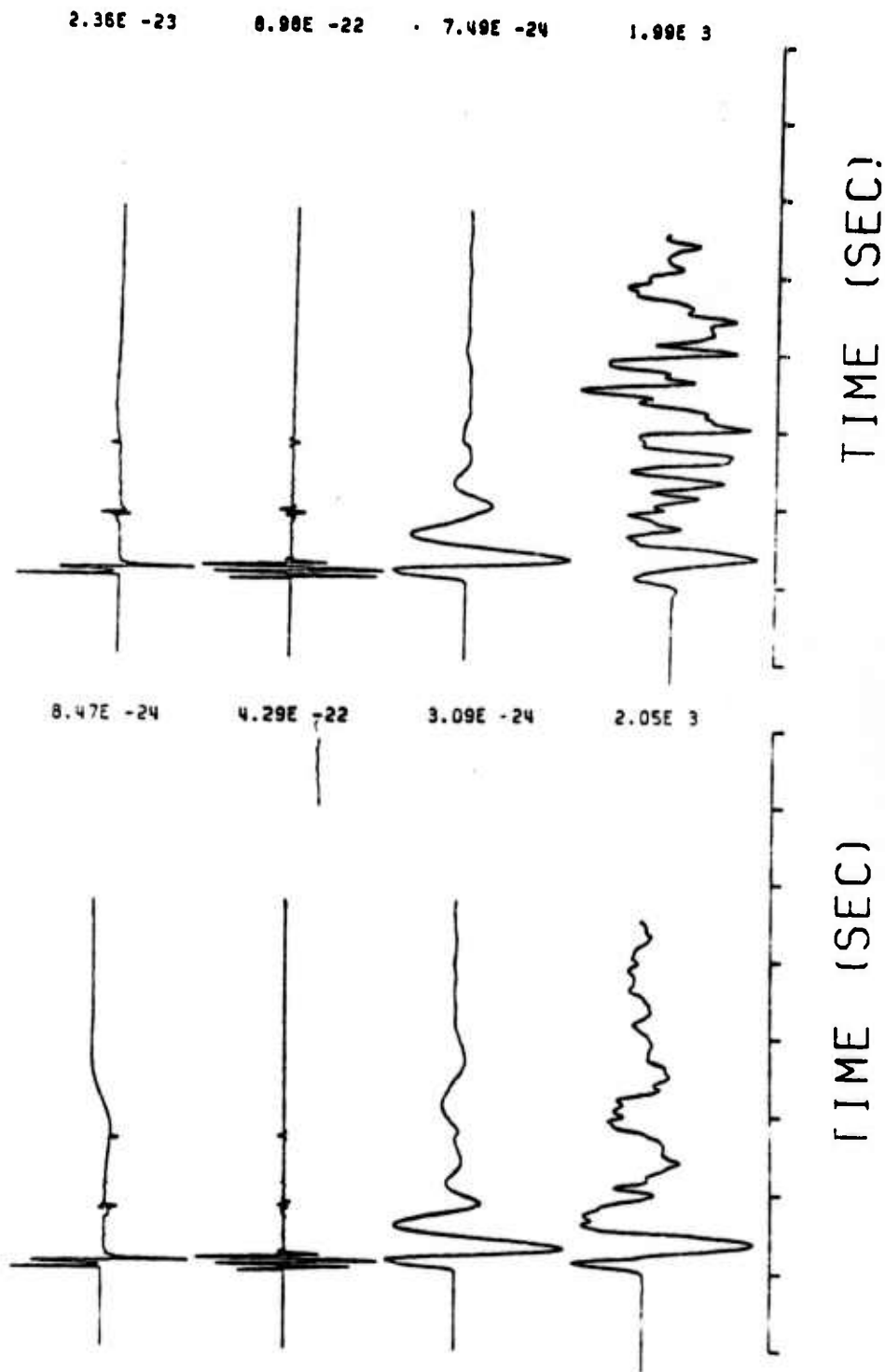


Figure 5.2. Comparison of theoretical with observed accelerograms taken on Nevada Test Site for the JORUM-HANDLEY explosions, vertical components on the left and radials on the right. For the case of a source within a single layer over a halfspace (center left of Figure 5.1), the top trace is theoretical ground motion from a step source pure explosion, the second trace is the result of passing the first through the accelerometer, the third includes source finiteness (0.6 second rise time and 1.05 to 1 overshoot), and the fourth is data.

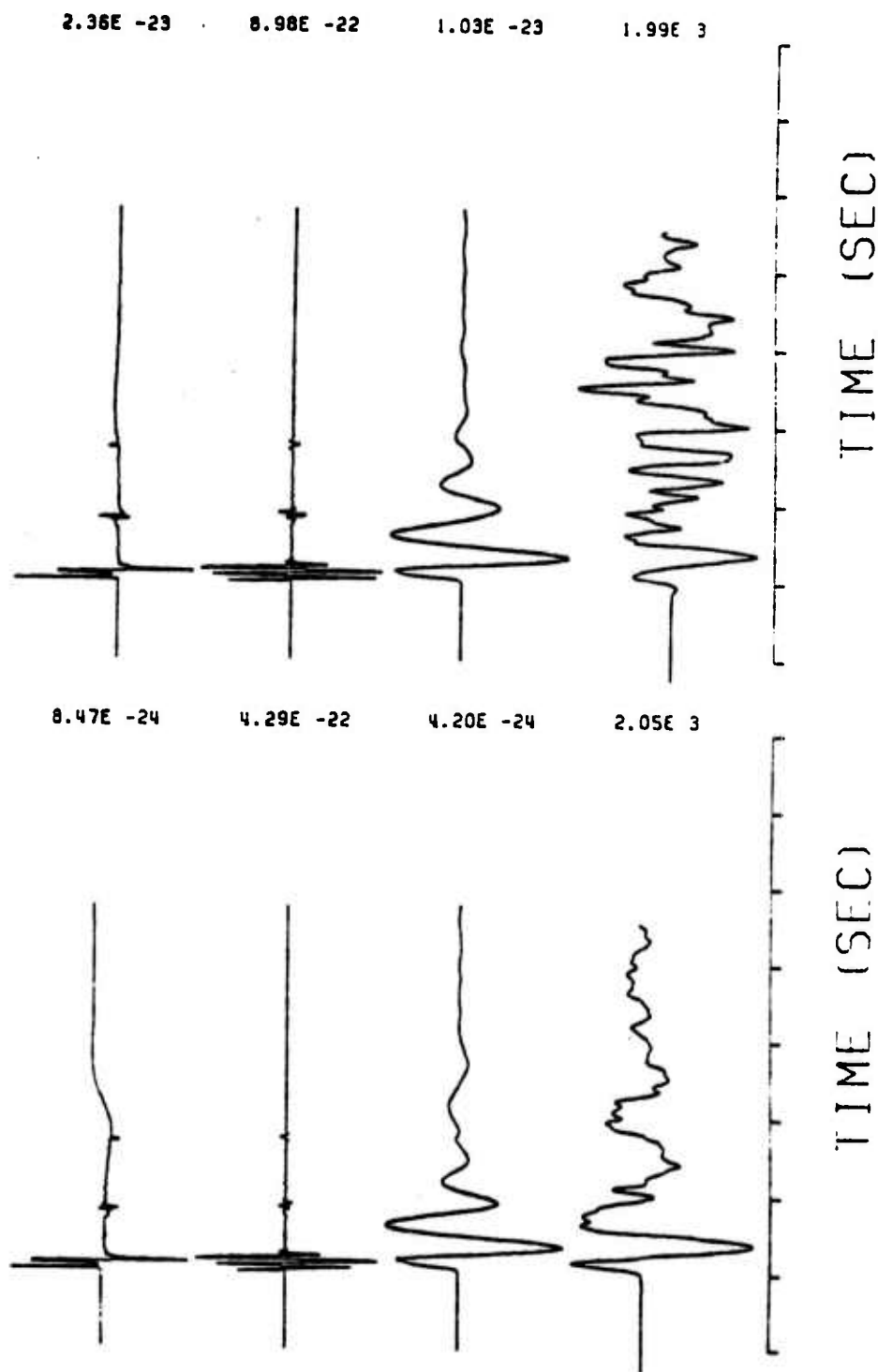
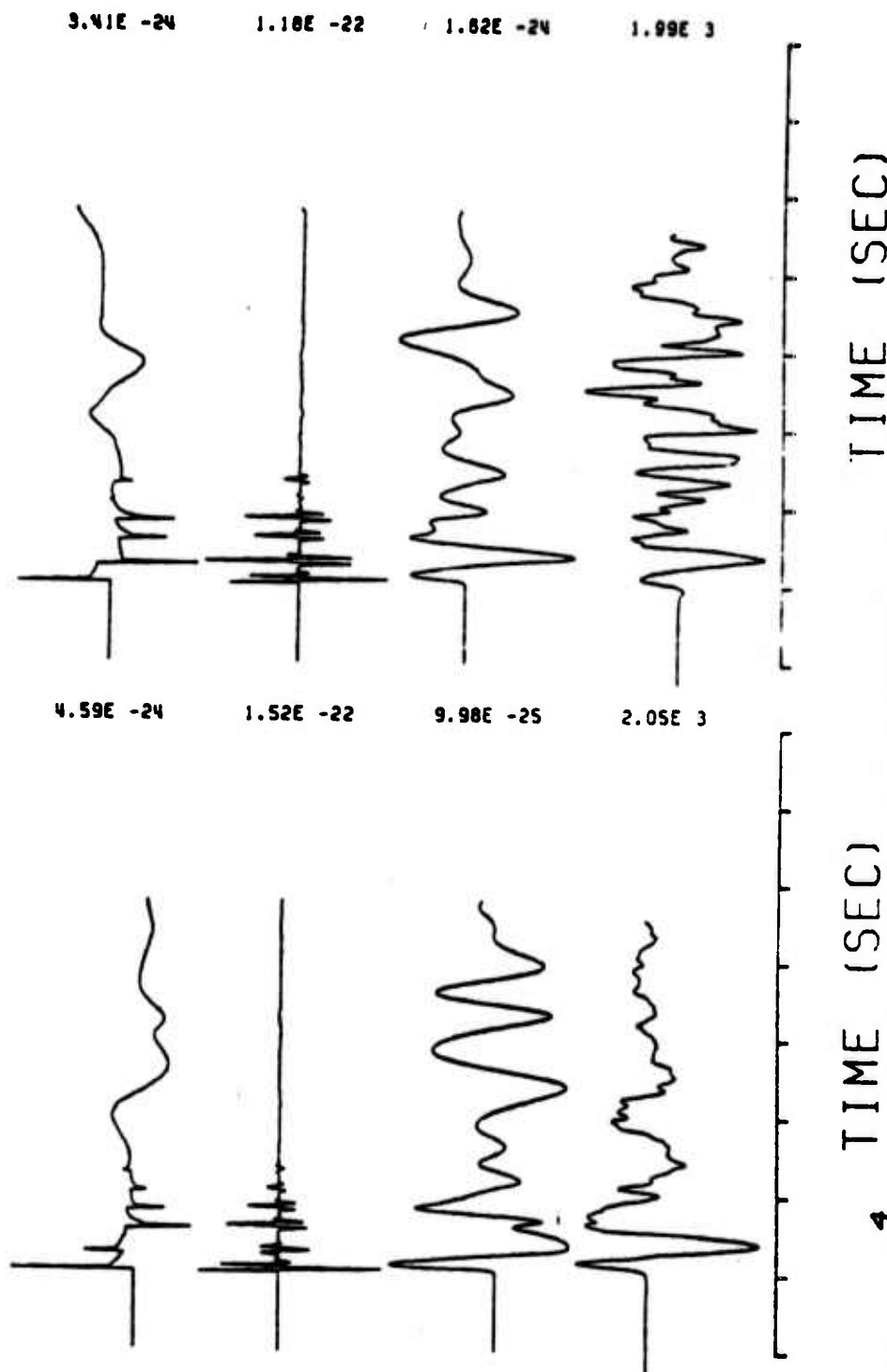


Figure 5.3. Same format as Figure 5.2 and same layer structure, but now the source has a 1.5 to 1 overshoot. Note that the P onset overshoots too much compared with Figure 5.2, which is a better fit.



4

Figure 5.1. Same format as Figure 5.2, but for the case of the source below the layer(right center model of Figure 5.1). Rise time of 0.6 second as before, and essentially no overshoot (about 1.0% to 1%).

the P onset. However, the vertical component synthetic looks only remotely like the data. The difference in signal character between the two synthetics is (probably artificially) caused by the sense of the P to S conversion; for the radial, this comes in about right, but for the vertical it is inverted relative to P (second spike of the top trace in Figure 5.4). Adding overshoot at the source did not help to improve the fit, nor did varying the rise time. What is shown is the best I could find for this layer model. Note the well-pronounced near-field effects on the top traces (the long-period trends in the trace before the surface wave).

5.3. Helmberger-Hadley model

I computed Green's functions for the Helmberger-Hadley (1980) model of the test site (Figure 5.1 bottom), summing direct, first-order reflections, and free-surface reflections. The resulting Green's functions can be seen in Figure 5.5. As can be seen the fit is quite poor, and probably because our source is placed in the third layer rather than the second. We would have hoped for a better comparison with Helmberger and Hadley, and the failure to attain this may be caused by: (1) the fact that our fit is done in acceleration and theirs is in velocity, (2) the different shape of our source time function, or (3) an error in the computation of the Green's function. During the next contract period I will conduct some definitive checks with existing generalized-ray codes from other groups, although I doubt that the MEXEC code can be grossly in error at this point.

5.4. Extended Helmberger-Hadley model

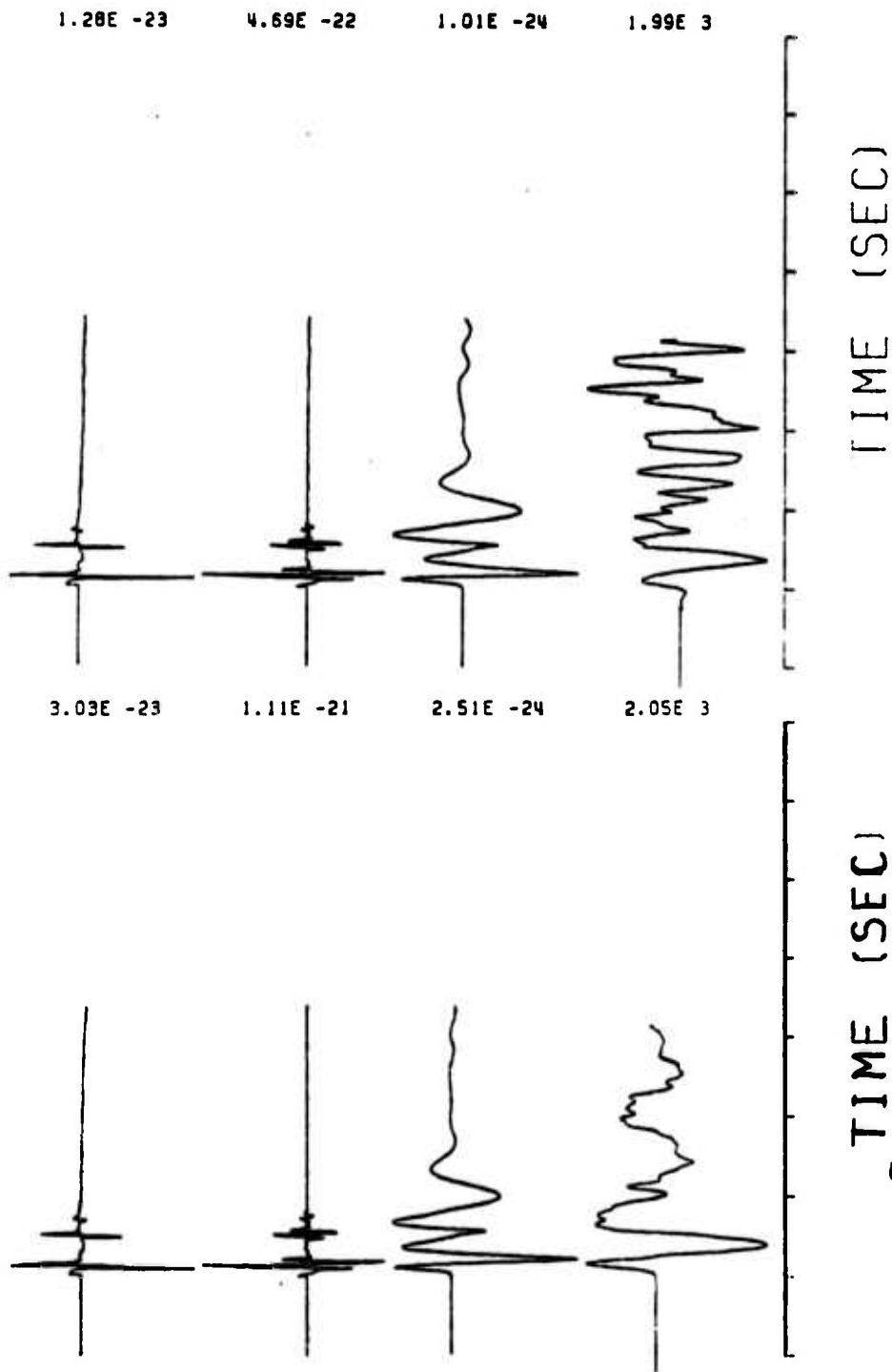
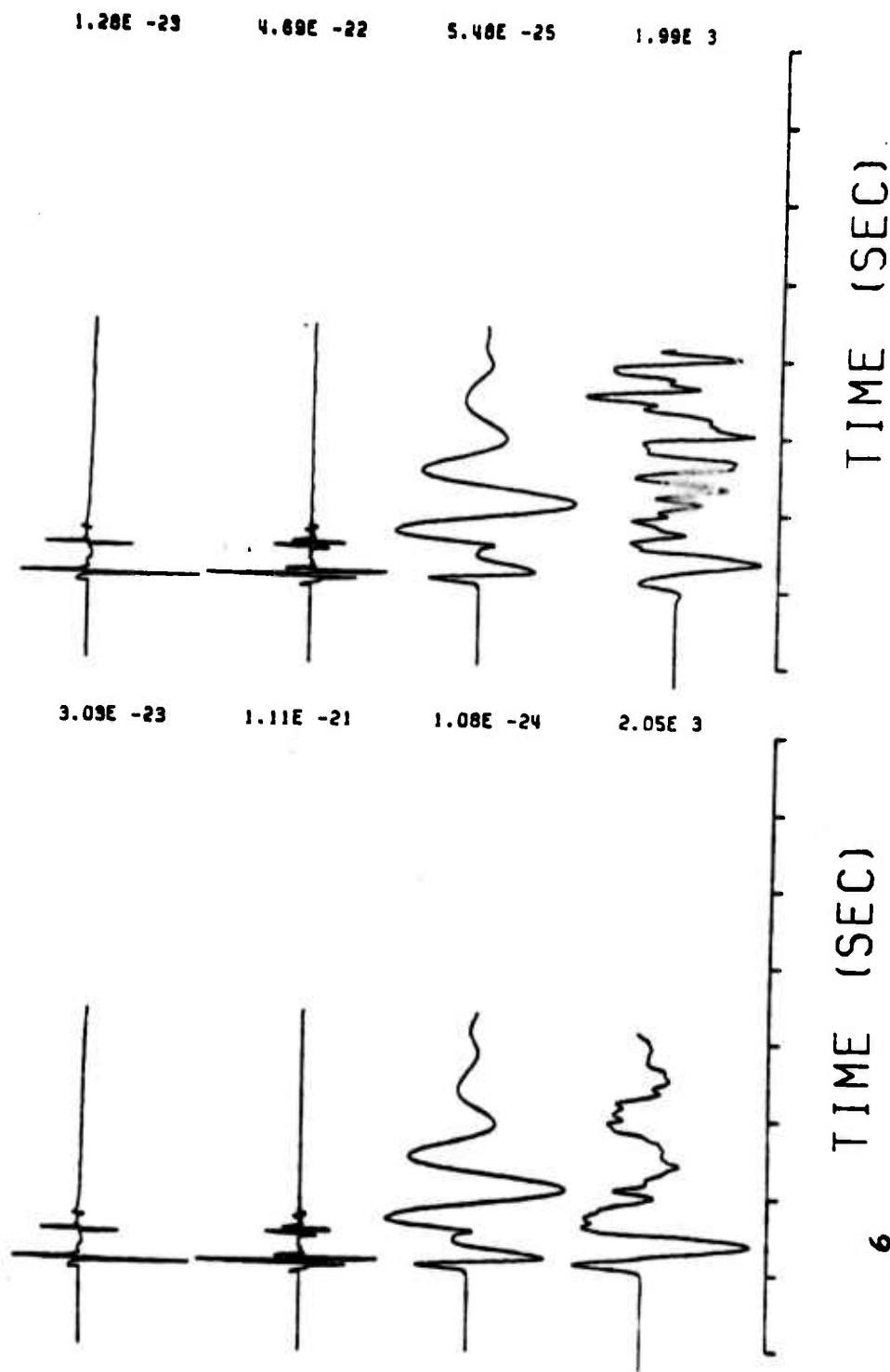


Figure 5.5. Same format as Figure 5.2 for the Helmburger-Hadley model (lower one in Figure 5.1). The source has mild (1.05 to 1) overshoot and a rise time of 0.6 second.



6

Figure 5.6. Same format as Figure 5.2 for the Helmlinger-Hadley model, but now the overshoot ratio is increased (1.5 to 1) and the rise time is 0.8 second.

It is known (e.g., Rodean, 1971) that the source of a nuclear explosion is no way a point source. Thus, all of the above studies which have employed this in the model violate known physics. In the previous subsections we have seen how critical the appearance of the Green's functions depends on the placement of the source, whether in the top, second, or third layer. To insure that the Green's functions are not dominated by this (arbitrary) placement in the layer stack, we must find some rational way to account for the source finiteness.

I have here used a crude but reasonable approach. Suppose a source radius of 0.5 km following Peppin (1977). Then the source will extend from the top of the second layer to the bottom part of the third one (see bottom image of Figure 6.1). Thus, replace the point source by a pair of point sources, one midway through the second layer and one at a depth of 1.53 km in the third layer. Scale these sources by the product of the volume in the respective layers and the rigidity of the layers, so that 27% is in the second layer and 73% is in the bottom layer (deltas in Figure 6.1 show the locations of these sources). Results are presented in Figure 6.7. The fit is still poor, but a little better than the fit obtained in the previous section.

It seems clear that the synthetics are most like the data when the source is placed in the second (not top or third) layer. In contrast to the statements of Peppin (1977), it is also clear that we need not resort to compound sources to fit these observations, an explosion will do very nicely. Of note is that the synthetics for earthquakes look nothing like the data for any of these models; Figure 5.8 is typical. Here we show the response to be expected from a dipslip earthquake placed at the same source depth as the explosions. Energy in the S and surface waves dominates the synthetics, and in particular dominates

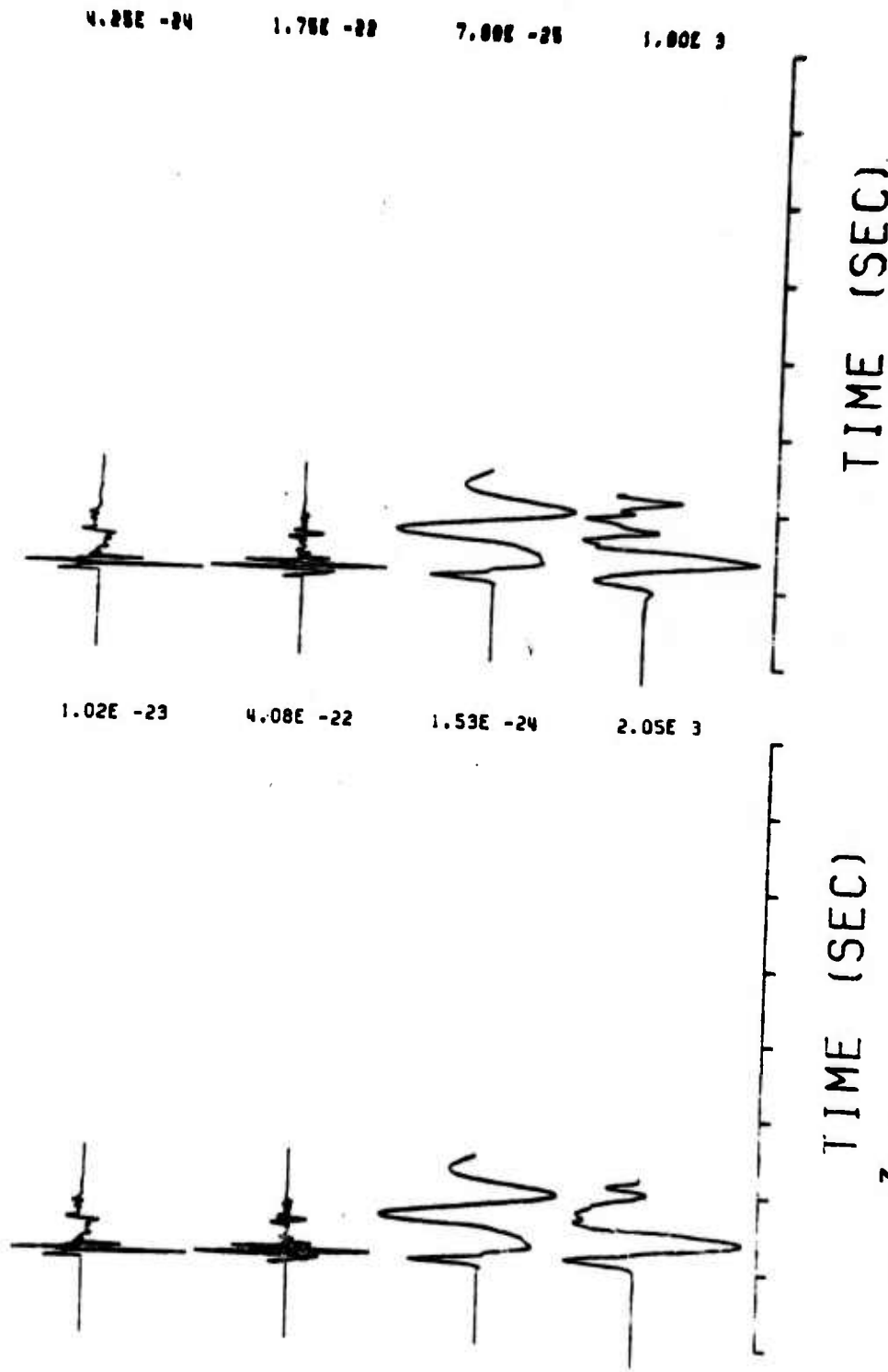


Figure 5.0⁷. Same format as Figure 5.2 for the extended Helmlinger-Hadley model. Rise time of 0.6 second and overshoot of 1.05 to 1.

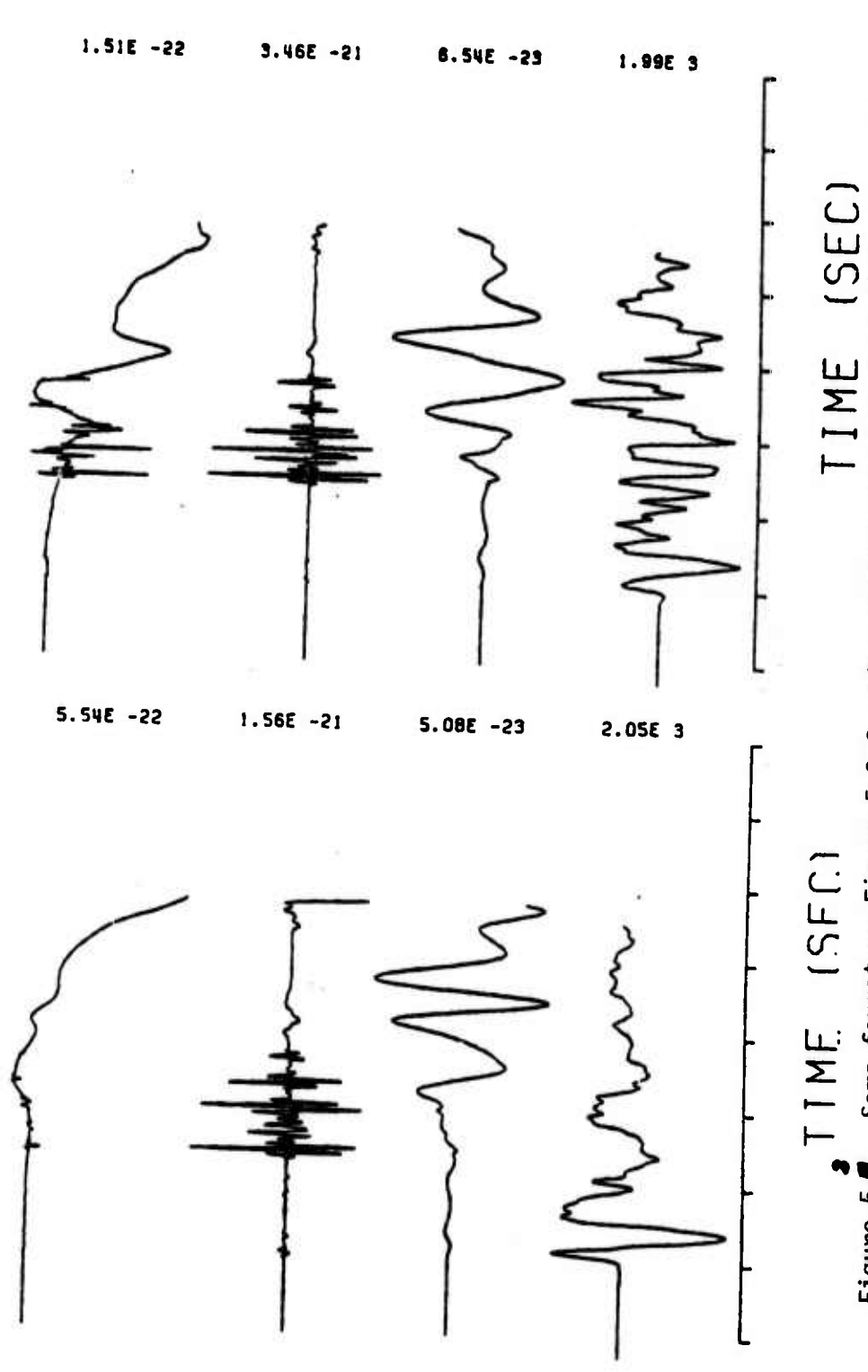


Figure 5.1. Same format as Figure 5.2 for the source under a layer (right-center model of Figure 5.1). This is for a dipslip earthquake source, vertical on the left and radial on the right.

the P arrival. It is certain that moment tensor inversion on any of these Green's functions will result in a source dominated by the isotropic (i.e., explosive) part. That is the most important question to explore in evaluating the moment tensor inversion method.

All of the Green's functions and data shown in this section are on the Cyber 176 computer at Kirtland Air Force Base in Albuquerque awaiting input to Brian Stump's moment tensor inversion code.

6. PN DISCRIMINATION IN A SHIELDLIKE ENVIRONMENT

An effort has been made during this contract period, through phone communications and a visit, to obtain data from St Louis University on the deep Merriam mine blasts of northern Missouri. These provide some of the most provocative data for seismic discrimination in existence, as the blasts are large (fraction of a kiloton) and recorded clearly out to ranges of hundreds of km. Records of these blasts, fired 3 km underground, are striking in the large S-waves present; they would be classified as explosions using the S/P discriminant discussed in Section 3, looking very much like local earthquakes indeed. Thus, this data should provide another severe test of the moment tensor analysis method. PN data is available on a dozen or so stations to the south and east of these blasts, as well as for some nearby earthquakes for comparison. I have attempted to obtain this data for investigation of PN discrimination as described in Section 4 of this report.

Due to limitations in staff and equipment at St Louis, the logistics of this effort are complicated and fairly expensive. We must rent dual tape play-

back systems at considerable cost and have these shipped to St Louis for transfer of the analog data to dub tapes. This will add a significant expense to this contract, of the order \$2,000. The data will be digitized and processed here on the Seismological Laboratory computer system sometime after the first of the year.

7. PERIPHERAL STUDIES OF INTEREST TO THIS CONTRACT

In this section is described work that is off the major emphasis of this contract, but nevertheless is relevant. We describe efforts aimed at acquisition of high-quality close-in data for earthquakes, a problem on earthquake spectral corner frequencies, and the use of explosions for the determination of phase velocity on the test site.

7.1. Digital data Acquisition and Spectral Corner Frequencies

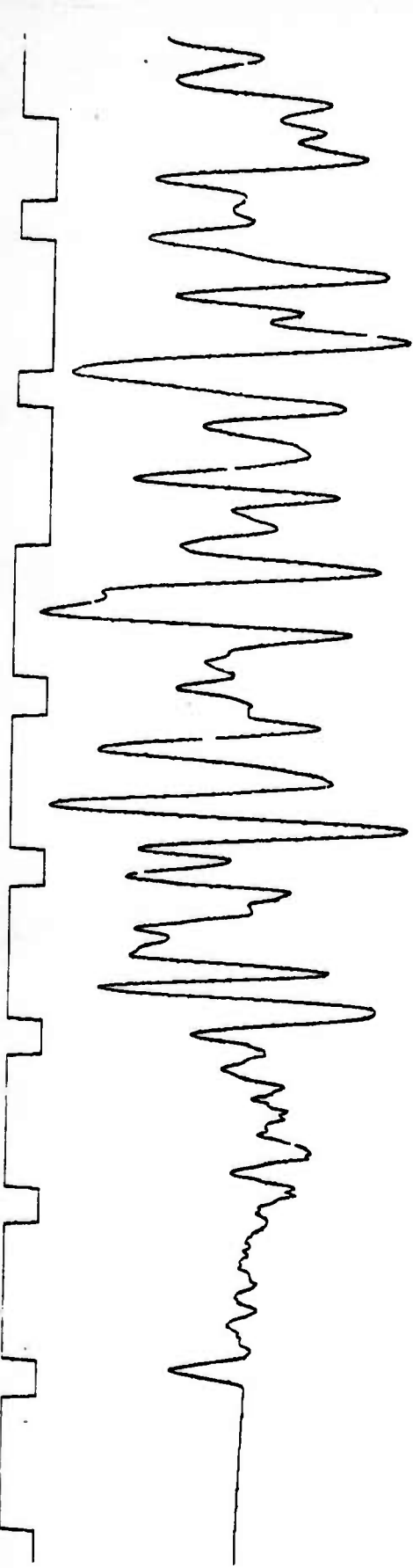
Over the past year and a half, I have, when time permits, attempted to continue our program of data acquisition using the high-quality digital event recorders built in 1976 and 1977 with support from AFOSR. These instruments have by now gone far in meeting the objectives of the Near-Field Project sponsored by the Air Force in the early 70s. We now have about 1,000 records of earthquakes in the Sierra and Great Basin region, many of unprecedented quality. This effort has become timely in view of the significant sequence of earthquakes which have been occurring in the Sierra Nevada boundary zone. The records obtained include many when the system was running flat in seismic displacement from 10 seconds to 50 Hz, extremely wide band for a portable system. The system has proven capable of fulfilling the design requirements of the Near-Field Project;

an earthquake of magnitude 3.3 recorded directly under the recorder was within full scale by a factor of 6: see Figure 7.1.

The acquisition has lead to a number of papers including one involving this author (Somerville et al., 1980). In this paper we discuss seismotectonics of the conspicuous Genoa-Carson fault system. In response to the occurrence of a sequence on the south end of this zone, we placed a digital event recorder almost directly over the source of the earthquakes, which was found to be a tight cluster 2 km in extent and 10 km deep. In Figure 7.2 we show a typical record obtained for an earthquake of about magnitude 1.5. Note the extreme complexity of the records for the nearly vertical wave propagation.

The major relevance of this work to source theory (hence, e.g., better understanding of seismic discrimination), is in further documentation of the rather enigmatic behavior of the ratio "R" of P to S-wave spectral corner frequencies. Shown in Figure 7.3 are the results of the Diamond Valley study, showing large (2.5) values for this ratio. Of interest is that this seems typical for other earthquake sequences recorded in the Sierra boundary zone. The result is not to be expected. Peppin and Simila (1976) studied earthquakes from the same region at the wideband Jamestown station, which entails propagation across the Sierran batholith, presumably a path with minimal attenuation. They found nearly unit values for R. That is, more P-wave energy is evident at the close-in stations than is evident at the more distant stations.

It seems unlikely that this can be the result of anelastic attenuation, since most work indicates that S energy attenuates as least as rapidly as P energy. If it is a source effect, then it seems puzzling that we again see about



Z

2976.



R

6656.

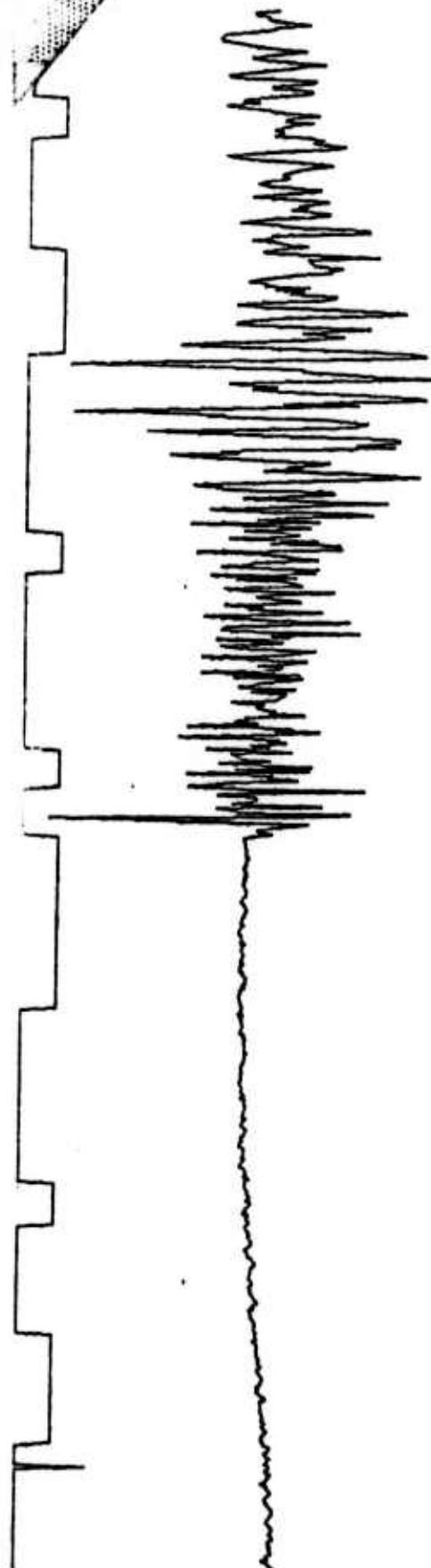


T

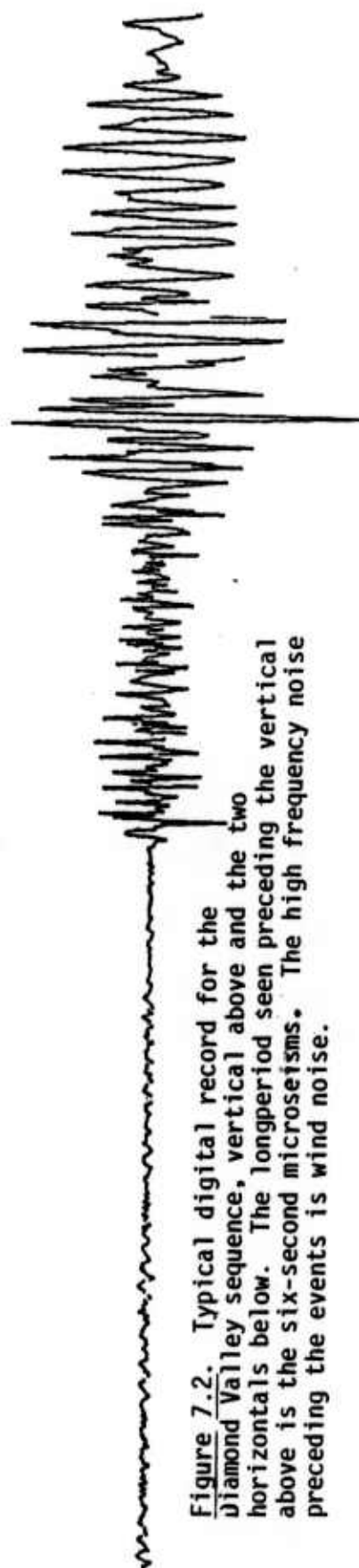
5568.

Figure 7.1. Wideband displacement records taken almost directly over an earthquake of magnitude 3.3, vertical component on top and the two horizontal components on the bottom. Numbers left are amplitude in digital counts, and the trace above is MWVB time code.

TEST . DAT



2992.
Z

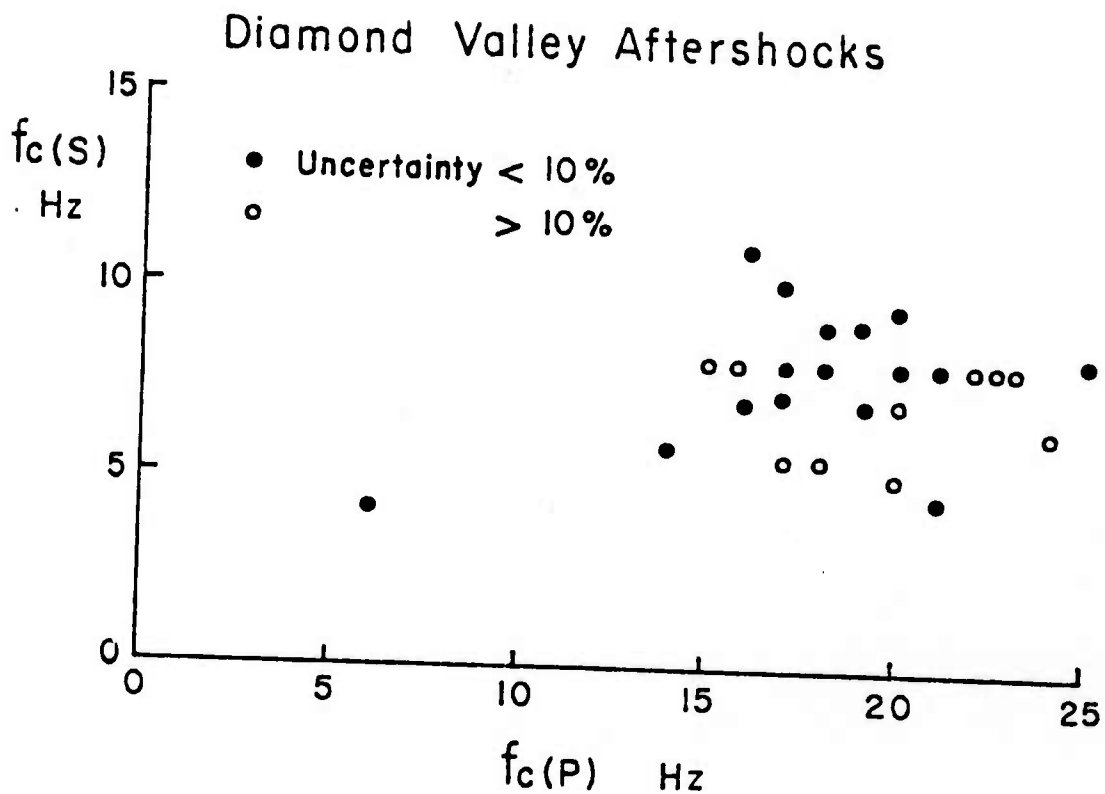


5456.
E

Figure 7.2. Typical digital record for the Diamond Valley sequence, vertical above and the two horizontal below. The longer period seen preceding the vertical above is the six-second microseisms. The high frequency noise preceding the events is wind noise.



3200.
Z



3

Figure 7.1. Plot of the ratio R of P-wave to S-wave spectral corner frequency for the Diamond Valley sequence. The P corner frequencies are a factor of 2.5 higher than the S corner frequencies.

unit values for the ratio R in the case events recorded at comparable distances near The Geysers, California: see Figure 7.4 from Peppin and Bufe (1980), using identical instrumentation and processing as was used to obtain Figure 7.2 for the Diamond Valley earthquakes.

In recent source theories the ratio R proves to be a strong diagnostic as to the nature of rupture propagation at the source. The results we have presented here, and others we are preparing for five other sequences in the Sierra province, may be leading to an important result either in terms of knowledge of the source or in terms of wave propagation and attenuation in the lower crust and upper mantle of the Basin and Range.

7.2. Analysis of Explosion Surface Waves for Phase Velocity

The existence of ultralong period data at the Berkeley array of wideband seismometers permits investigation of phase velocity over short paths on the test site. To complement the work of Priestley and Brune on surface wave analysis in the Basin and Range, I have studied some of the large explosions recorded at Berkeley and Jamestown. Data quality is excellent, showing clear energy in the surface wave spectrum of explosions out to periods of 100 seconds. An idea of the data quality can be obtained by reference to Figure 7.6, showing records of the COLBY test taken on the wideband system at Jamestown. Note factor-of-ten signal power above the noise out to frequencies of 50 Hz.

The idea of the method employed here was to use two explosions on the test site as recorded by a single station (Berkeley or Jamestown). The difference in phase between similar surface wave packets of explosions along a line of azimuth

4
 Figure 7.1. Ratio of spectral corner frequencies of P and S waves for events recorded at The Geysers, California, with induced events presumed at the steam site and natural earthquakes off that site.

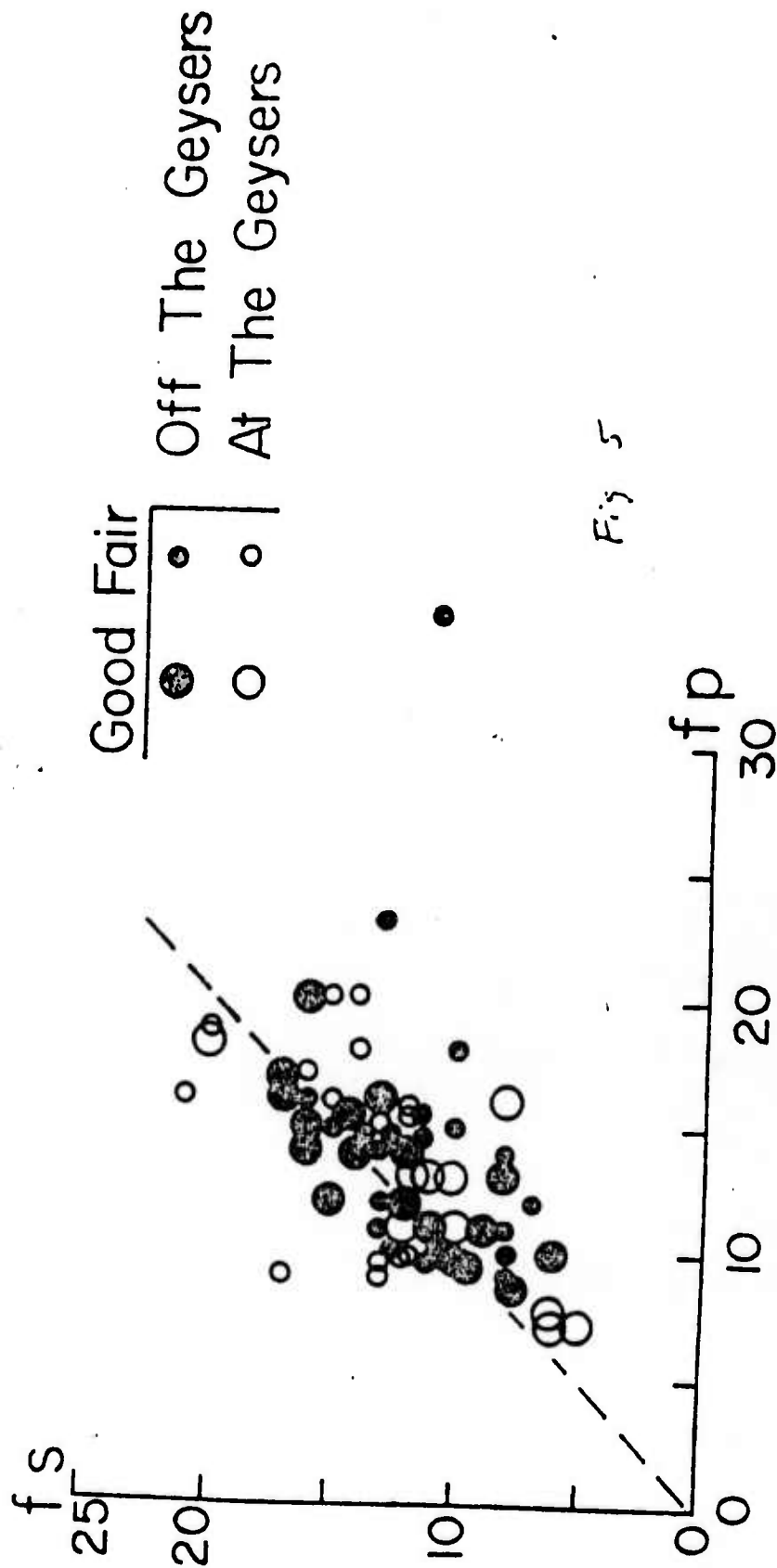
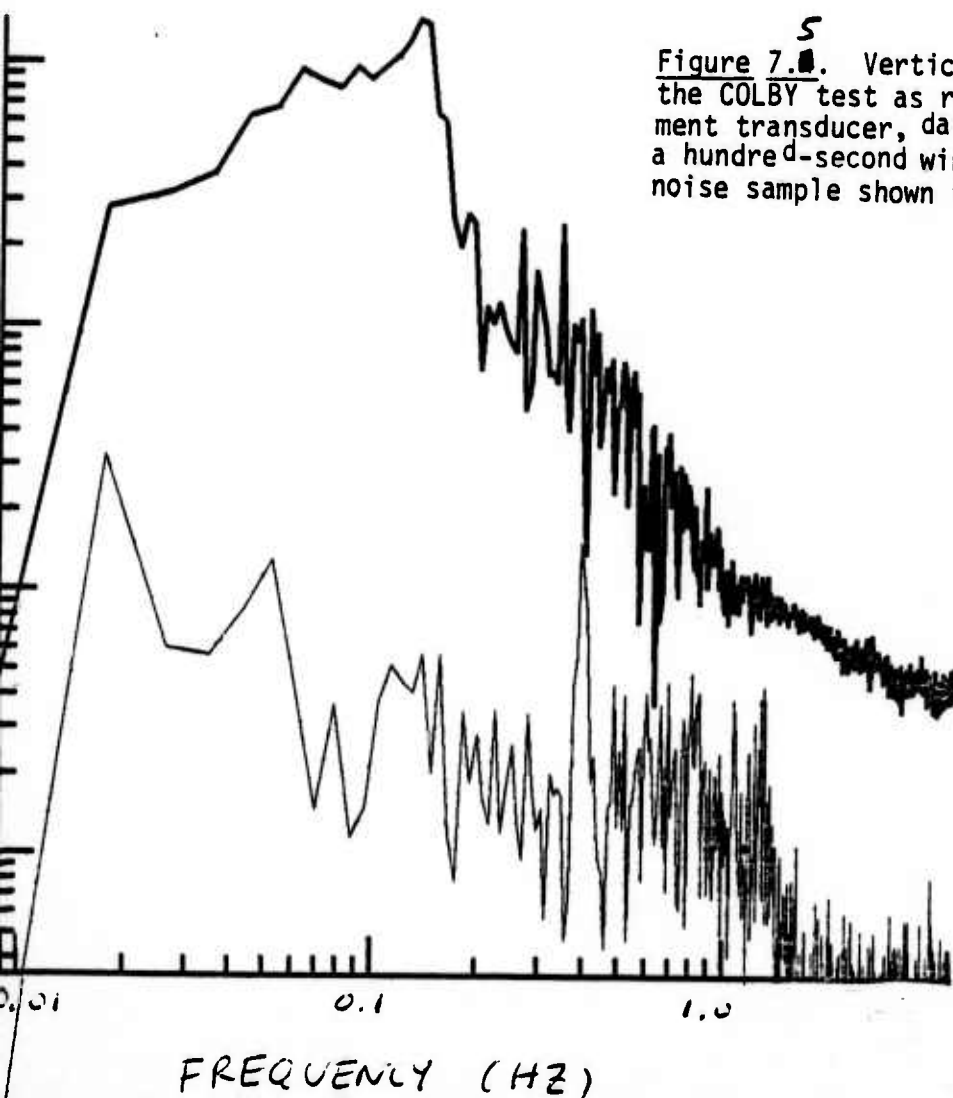
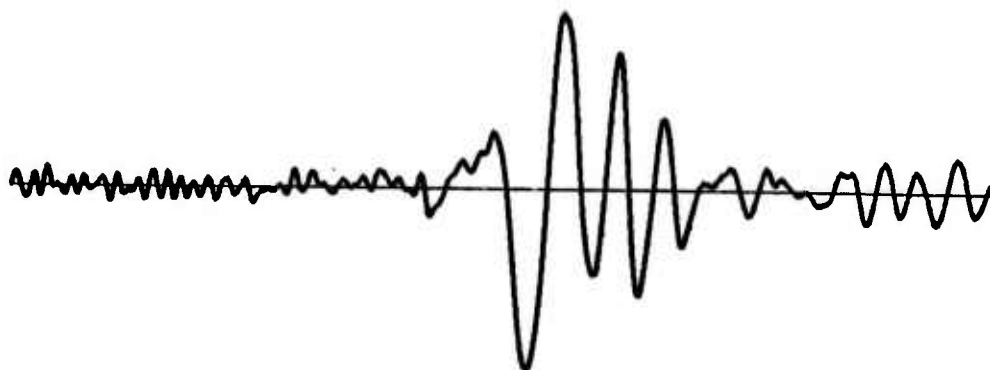


Fig 5

COLBY AT JAS



⁵
Figure 7.4. Vertical-component surface waves for the COLBY test as recorded on the Jamestown displacement transducer, data shown above. A spectrum with a hundred-second window was computed below, with a noise sample shown in lighter line weight.

DK1:MUMENTEST.DAT

T	U
30.0	3:01
33.0	3:01
36.0	3:00
39.0	3:08
42.0	3:07
45.0	3:05
48.0	3:04
51.0	3:04
54.0	3:03
57.0	3:03
60.0	3:02

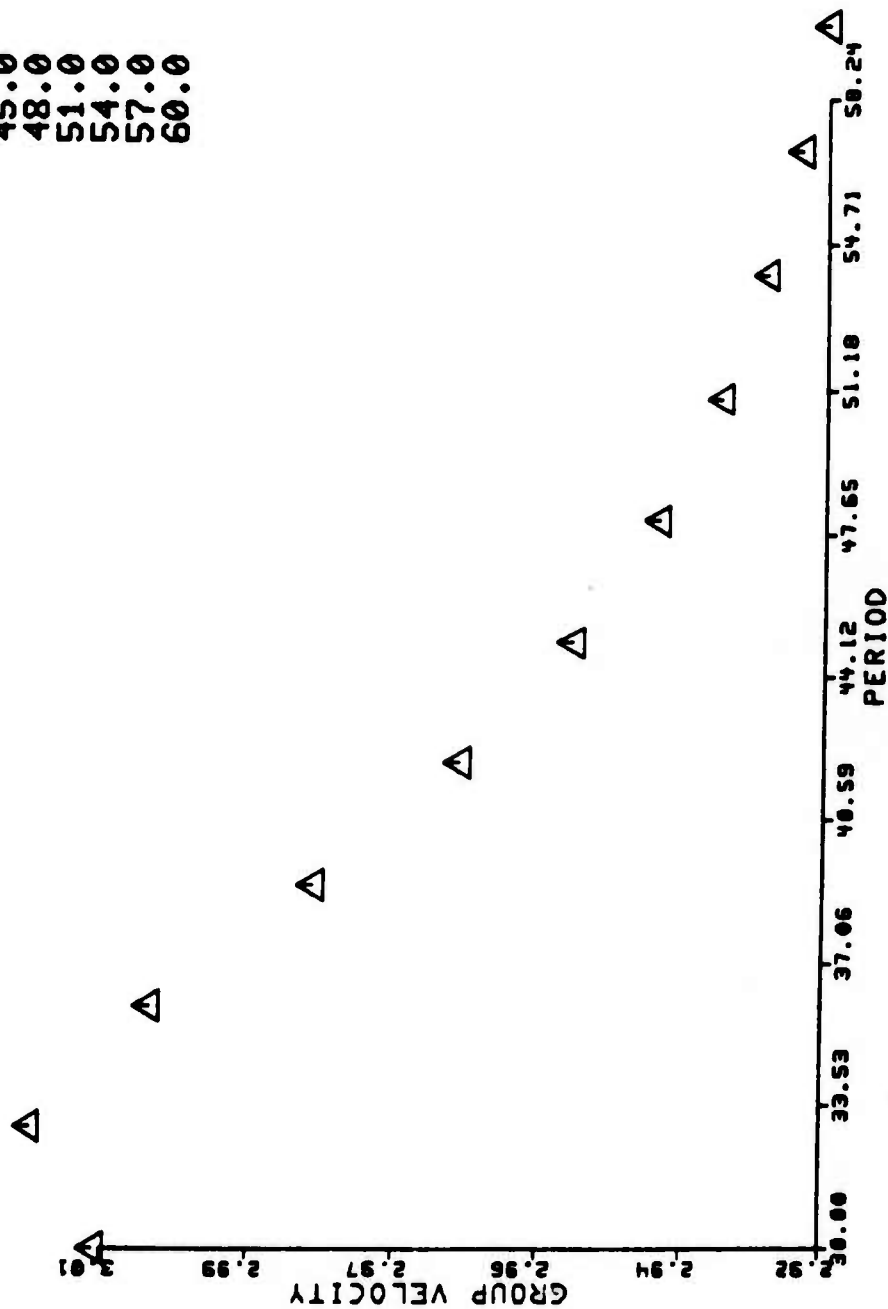
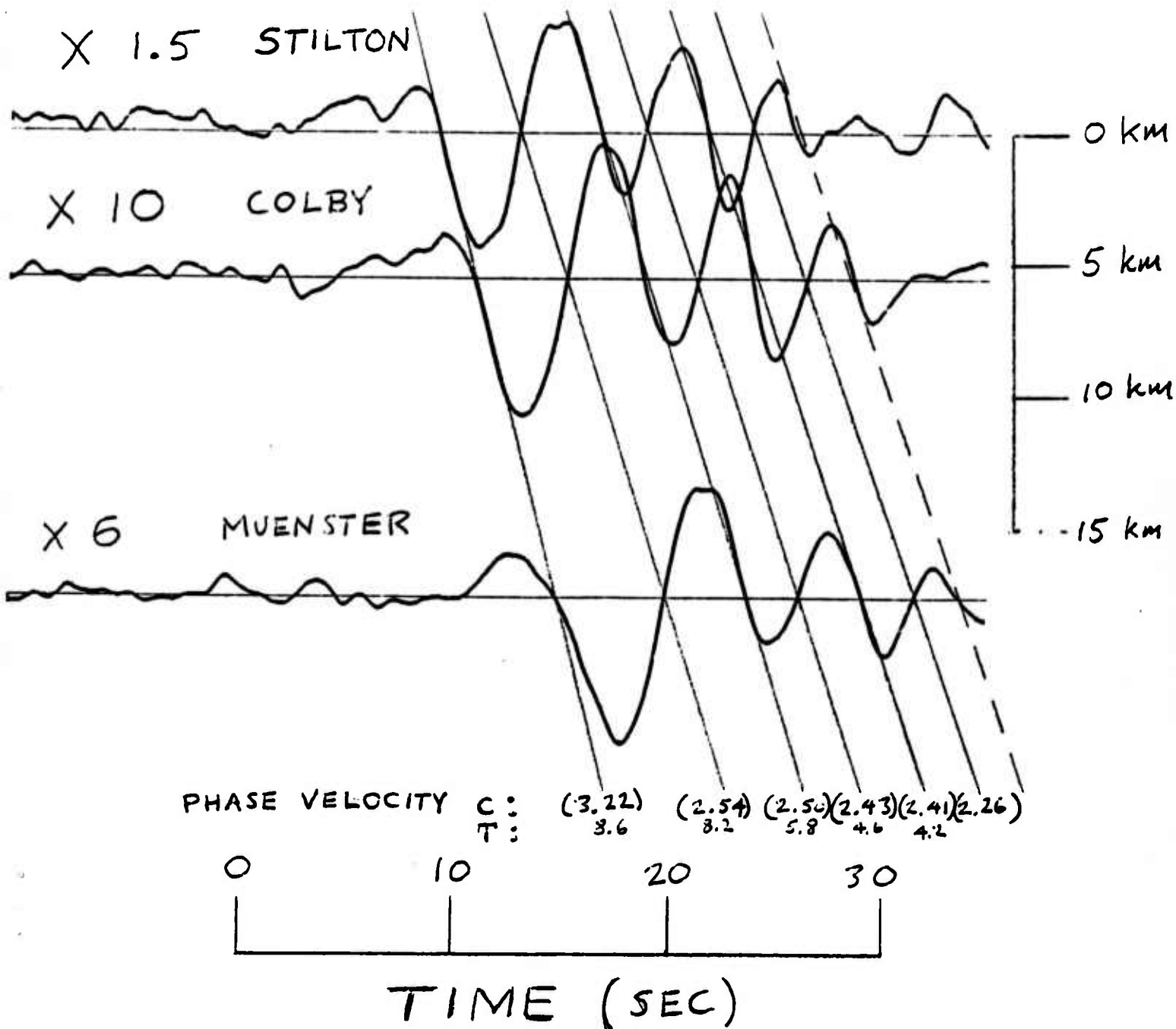


Figure 7.6. Group velocity of 30 to 50-second surface waves at Jamestown for the MUMENTEST test.

PAHUTE EVENTS - JAS



⁷
Figure 7.0. Three shots on almost exactly the same azimuth line from the test site to Jamestown, with trace separation proportional to the separation of the respective shotpoints. Visual correlations used to compute phase velocity in the 4.2 to 8.6 second range.

(44.9"
window)

PAHUTE EVENTS - BRK

X 6 COLBY

0 10 20 30
TIME (SEC)

X 6 MUENSTER

8
Figure 7.8. Same format as Figure 7.6 for the large tests MEENSTER and COLBY as recorded on the Berkeley ultralong period system, vertical component. Periods out to 100 seconds can be seen easily in the spectral records of these data.

$c = 3.03$
 $T \approx 25''$

gives rise to a measurement of the structure underneath the zone between the two paths, in this case extending to the bottom of the crust or even deeper. While phase resolution is reduced because of the short paths used, we gain the advantage of precise determination of phase velocity (in theory) for areas of interest on the test site. Group velocity analysis was attempted first on the records to see how well the signals were dispersed; see a typical result in Figure 7.6. For the MUENSTER test, the information extends to 60 seconds.

The program to invert for phase velocity was not successful. However, in Figures 7.7 and 7.8 the phase moveout can clearly be seen for combinations of explosions; the surface wave packets of the different explosions look very similar indeed, and phase correlation is easy to do visually. Our aim is to extend and overlap the extensive data set of Priestley and Brune, hopefully to 40 seconds, with emphasis for paths on the test site. A cooperative effort with a graduate student at Berkeley was initiated during this contract period for the purpose of pursuing this effort.

REFERENCES CITED

- Bakun, W. H. and L. R. Johnson, 1970. Short period spectral discriminants for explosions, Geophys. J. R. A. S., 22, 139-152.
- Burridge, R. and L. Knopoff, 1964. Body force equivalents for seismic dislocations, Bull. Seism. Soc. Am., 54, 1875-1888.
- Douglas, A., Hudson, J. A. and V. K. Kambhavi, 1971. The relative excitation of seismic surface and body waves by point sources, Geophys. J. R. A. S., 23, 451-460.
- Johnson, L. R. and T. V. McEvilly, 1974. Near-field observations and source parameters of central California earthquakes, Bull. Seism. Soc. Am., 64,

1855-1886.

- Leet, L. D., 1962. The detection of underground explosions, Sci. Am., 206, 55-59.
- McEvilly, T. V. and W. A. Peppin, 1972. Source characteristics of earthquakes, explosions, and afterevents, Geophys. J. R. A. S., 31, 67-82.
- Murphy, J. R. and J. A. Lahoud, 1975. Analysis of Near-Field Ground Motion Spectra from Explosions and Earthquakes, ARPA Technical report from Computer Science Corporation, February.
- Peppin, W. A., 1974. The Cause of the Body Wave-Surface Wave Discriminant between Earthquakes and Underground Nuclear Explosions at Near-Regional Distances, Ph.D. Thesis, University of California, Berkeley.
- Peppin, W. A., 1977. A near-regional explosion source model for tuff, Geophys. G. R. A. S., 48, 331-349.
- Peppin, W. A., 1979. Analysis of close-in accelerograms of megaton explosions for source parameters, EOS, Trans. Am. Geophys. Un., 60, 895, Abstract.
- Peppin, W. A. and T. V. McEvilly, 1973. Discrimination among small magnitude events on Nevada Test Site, Geophys. J. R. A. S., 37, 227-244.
- Peppin, W. A. and C. G. Bufe, 1980. Induced versus natural earthquakes: search for a seismic discriminant, Bull. Seism. Soc. Am., 70, in press, February.
- Peppin, W. A. and G. W. Simla, 1976. P and SV-wave corner frequencies over low loss paths: a discriminant for earthquake source theories? Jour. Phys. Earth, 24, 177-188.
- Priestley, K. and J. N. Brune, 1978. Surface waves and the structure of Nevada and western Utah, Jour. Geophys. Res., 83, 2265.
- Rodean, H. C., 1971. Nuclear Explosion Seismology, U. S. A. E. C. Division of Technical Information.

- Somerville, M. R., Peppin, W. A. and J. D. VanWormer, 1980. An earthquake sequence in the Sierra Nevada-Great Basin boundary zone: Diamond Valley, Bull. Seism. Soc. Am., submitted for publication.
- Stump, B. W., 1979. Investigation of seismic sources by the linear inversion of seismograms, Ph.D. Thesis, University of California at Berkeley.
- Stump, B. W. and L. R. Johnson, 1977. The determination of source properties by the linear inversion of seismograms, Bull. Seism. Soc. Am., 67, 1489-1502.
- Viecellif, J. A., 1973. Spallation and the generation of surface waves by an underground explosion, Jour. Geophys. Res., 78, 2475-2487.

UNCLASSIFIED

SECURITY CLASSIFICATION OF THIS PAGE (When Data Entered)

REPORT DOCUMENTATION PAGE		READ INSTRUCTIONS BEFORE COMPLETING FORM
1. REPORT NUMBER 1	2. GOVT. ACCESSION NO. A156033	3. RECIPIENT'S CATALOG NUMBER
4. TITLE (and Subtitle) CLOSE-IN AND REGIONAL SOURCE STUDIES FOR SEISMIC DISCRIMINATION		5. TYPE OF REPORT & PERIOD COVERED ANNUAL 01 Oct 1978-31 Sep 1979
7. AUTHOR(s) William A. PEPPIN		6. PERFORMING ORG. REPORT NUMBER
9. PERFORMING ORGANIZATION NAME AND ADDRESS Seismological Laboratory Mackay School of Mines University of Nevada, Reno, 89557		8. CONTRACT OR GRANT NUMBER(s) F49620-77-C-0070
11. CONTROLLING OFFICE NAME AND ADDRESS James K. Murphy Office of the Controller University of Nevada, Reno 89557 NV		10. PROGRAM ELEMENT, PROJECT, TASK AREA & WORK UNIT NUMBERS
14. MONITORING AGENCY NAME & ADDRESS (if different from Controlling Office) Air Force Office of Scientific Research Bolling Air Force Base Washington, D.C. 20332		12. REPORT DATE 03 Dec 1979
		13. NUMBER OF PAGES 27
		15. SECURITY CLASS. (of this report) UNCLASSIFIED
		15a. DECLASSIFICATION/DOWNGRADING SCHEDULE
16. DISTRIBUTION STATEMENT (of this Report) UNLIMITED <div style="border: 1px solid black; padding: 5px; display: inline-block;">DISTRIBUTION STATEMENT A Approved for public release Distribution Unlimited</div>		
17. DISTRIBUTION STATEMENT (of the abstract entered in Block 20, if different from Report) UNLIMITED		
18. SUPPLEMENTARY NOTES		
19. KEY WORDS (Continue on reverse side if necessary and identify by block number) Seismic discrimination. Discrimination. Seismic source. Source. Moment tensor inversion. Theoretical seismograms. Surface wave analysis. Near-regional discrimination.		
20. ABSTRACT (Continue on reverse side if necessary and identify by block number) > Studies are conducted in a number of areas pertinent to seismic discrimination. Attempts are made to check the efficiency of the Pn-Rayleigh discriminant found by McEvelly and Peppin (1972); results are not favorable for the use of this discriminant. Rather, a discriminant based on the excitation of Pg and Sg (or Lg), investigated by others, is found to be quite effective. Analyses of close-in accelerograms is attempted with the view toward application of moment tensor analysis. Results show that recent studies are		

DD FORM 1 JAN 73 1473

EDITION OF 1 NOV 65 IS OBSOLETE

UNCLASSIFIED
SECURITY CLASSIFICATION OF THIS PAGE (When Data Entered)


UNCLASSIFIED

SECURITY CLASSIFICATION OF THIS PAGE(When Data Entered)

cont
(from 20) still in significant disagreement.

An attempt is made to investigate a seismic discriminant based on Pn alone. A set of Green's functions and data for small explosions have been assembled for application of moment tensor analysis.

Peripheral studies include source studies of Basin and Range earthquakes and a study of Rayleigh wave dispersion on the test site.



UNCLASSIFIED

SECURITY CLASSIFICATION OF THIS PAGE(When Data Entered)